Calorimeters – Upbringing & Care

A brief review on my personal journey from clean to dirty physics and the things we are trying to measure with the coolest detectors in the world

Peter Loch

Department of Physics
University of Arizona
Tucson, Arizona, USA

THE UNIVERSITY OF ARIZONA
UAPhysics
THE UNIVERSITY OF ARIZONA
College of Science

Calorimeters – Upbringing & Care

A brief review on my personal journey from clean to dirty physics and the things we are trying to measure with the ~~coolest~~ coldest detectors in the world

Peter Loch

Department of Physics
University of Arizona
Tucson, Arizona, USA

THE UNIVERSITY OF ARIZONA
UAPhysics
THE UNIVERSITY OF ARIZONA
College of Science

In the beginning…

1981 in the basement of the Physics Department of the University of Hamburg and I thought …

In the beginning…

… *this is a calorimeter!*

And it is!

… and now:

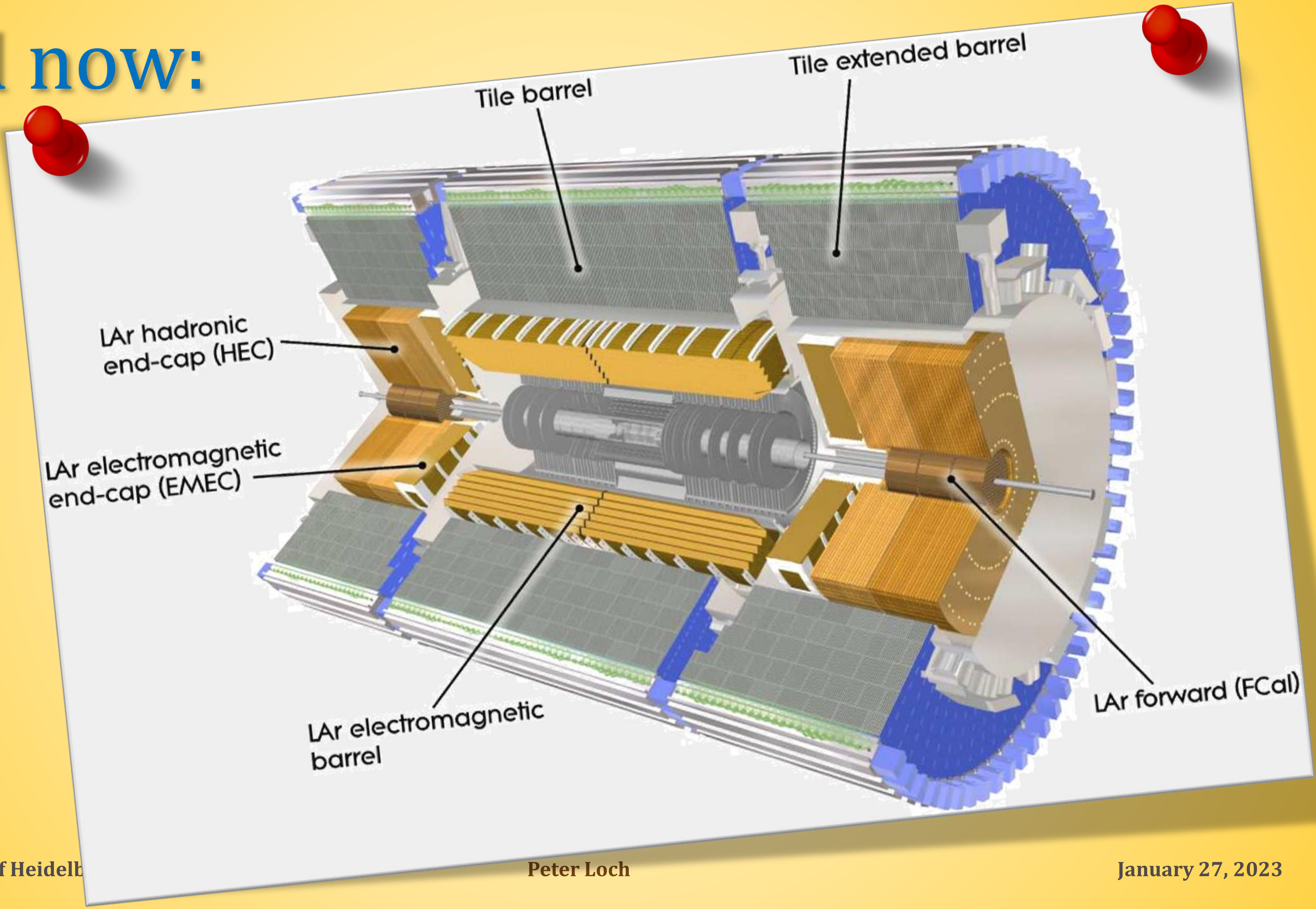
Tile barrel
Tile extended barrel
LAr hadronic end-cap (HEC)
LAr electromagnetic end-cap (EMEC)
LAr electromagnetic barrel
LAr forward (FCal)

GEANT4 Simulation: 10 GeV e^- in copper

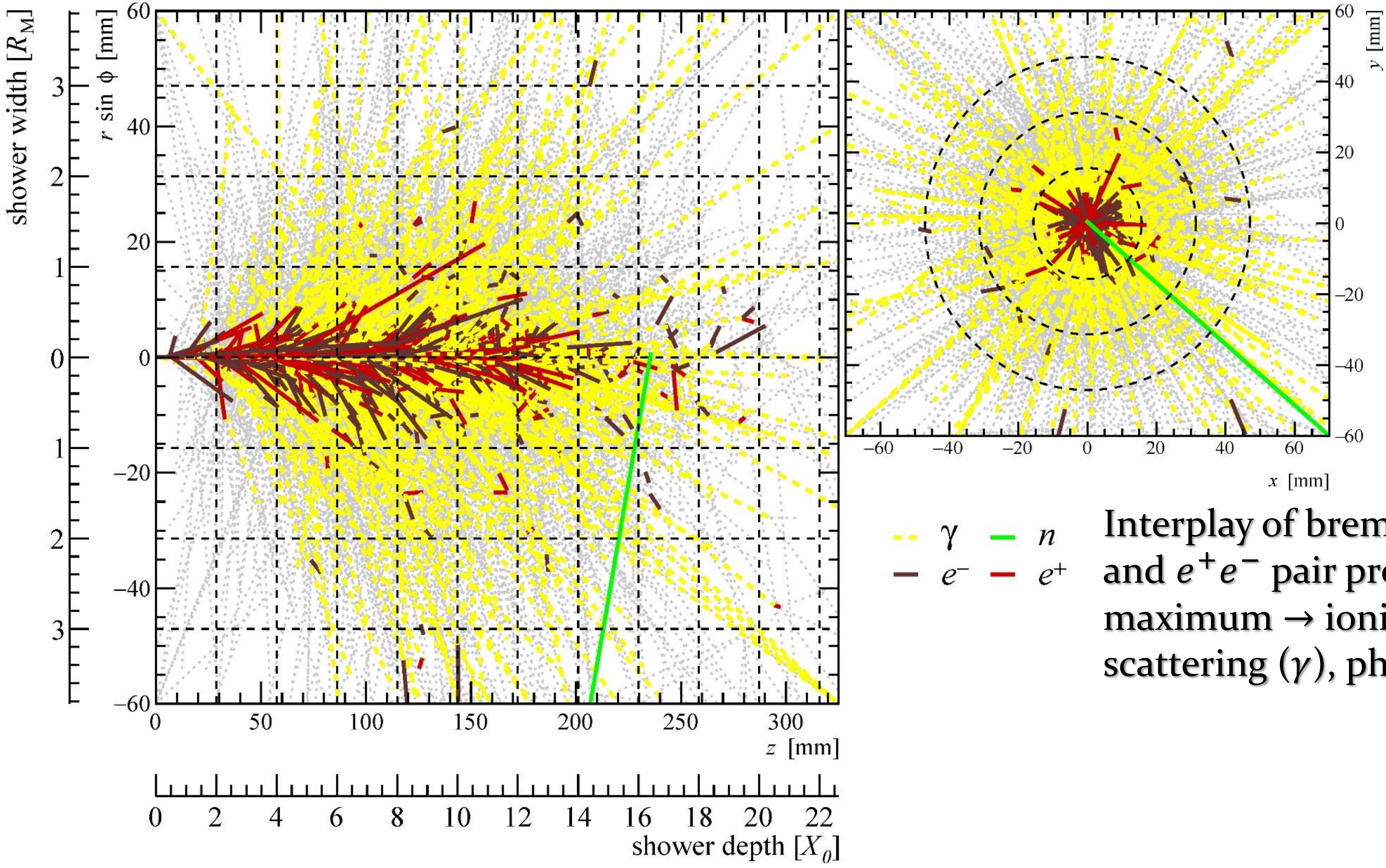

Interplay of bremsstrahlung and e^+e^- pair production up to shower maximum → ionizations ($e^{\pm}$), Compton scattering (γ), photo-effect (γ)

GEANT4 Simulation: 10 GeV e^- in copper

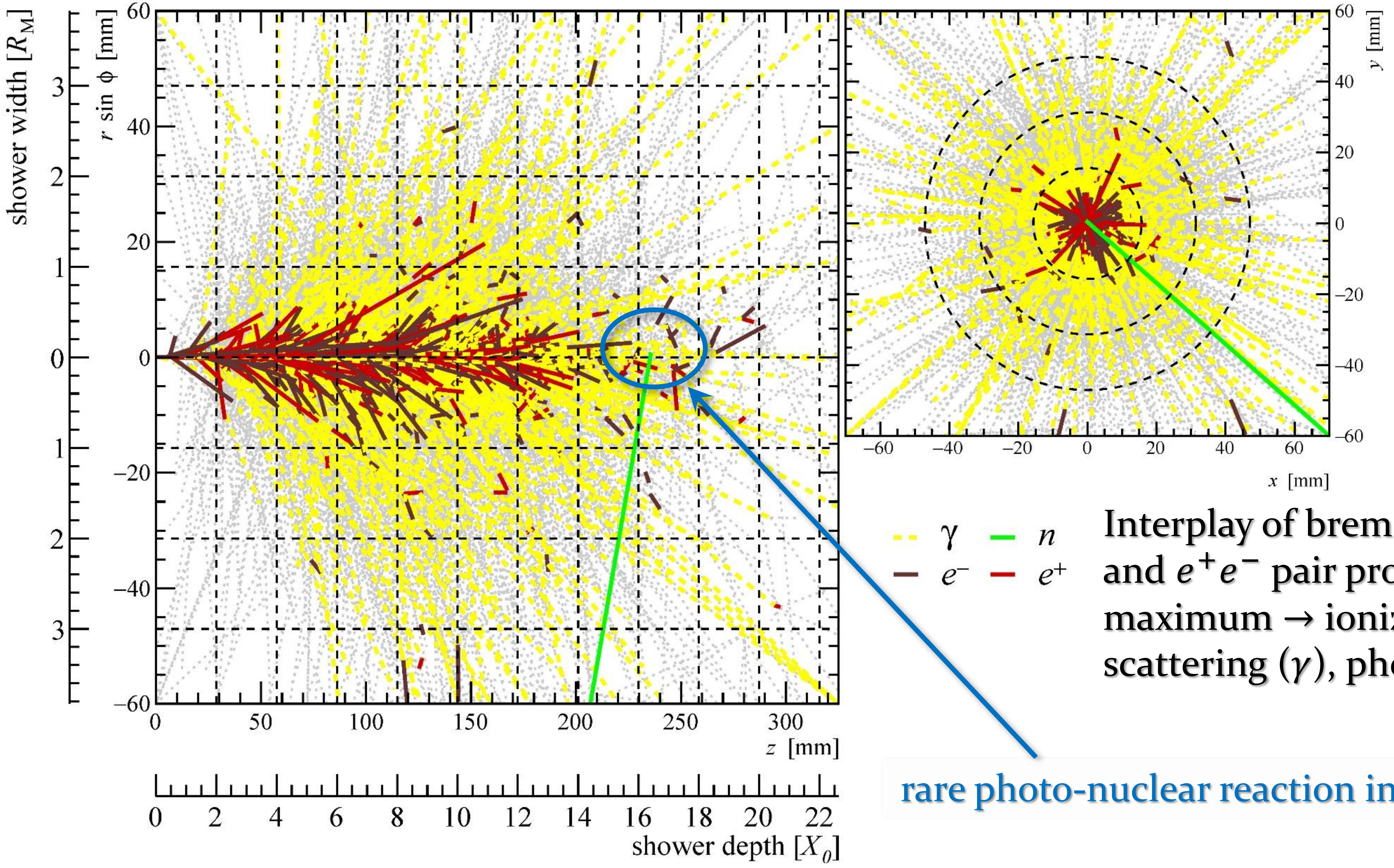

Interplay of bremsstrahlung and e^+e^- pair production up to shower maximum → ionizations ($e^\pm$), Compton scattering (γ), photo-effect (γ)

rare photo-nuclear reaction in EM shower

QCD drives fast shower development

- Hadron interacts with nucleon in nuclei
  - Like a fixed target collision
  - Develops intra-nuclear cascade (fast)
- Fast stage – hadron production in intranuclear cascade
  - Secondary hadrons escape nucleus
  - Neutral pions decay ~immediately into two photons → electromagnetic cascade
  - Other hadrons can hit other nucleons → inter-nuclear cascade
  - **Dominating signal contribution**

Slow de-excitation of nuclei

- Remaining nucleus in excited state
  - Evaporates energy to reach stable (ground) state
  - Fission and spallation possible
  - **Small signal contribution in ATLAS Tile calorimeter**
- Binding energy and low energetic photons
  - **Little to no signal contribution in ATLAS calorimeters**

Large process fluctuations

- ~200 different interactions
- Highest probability process ≈ 2%

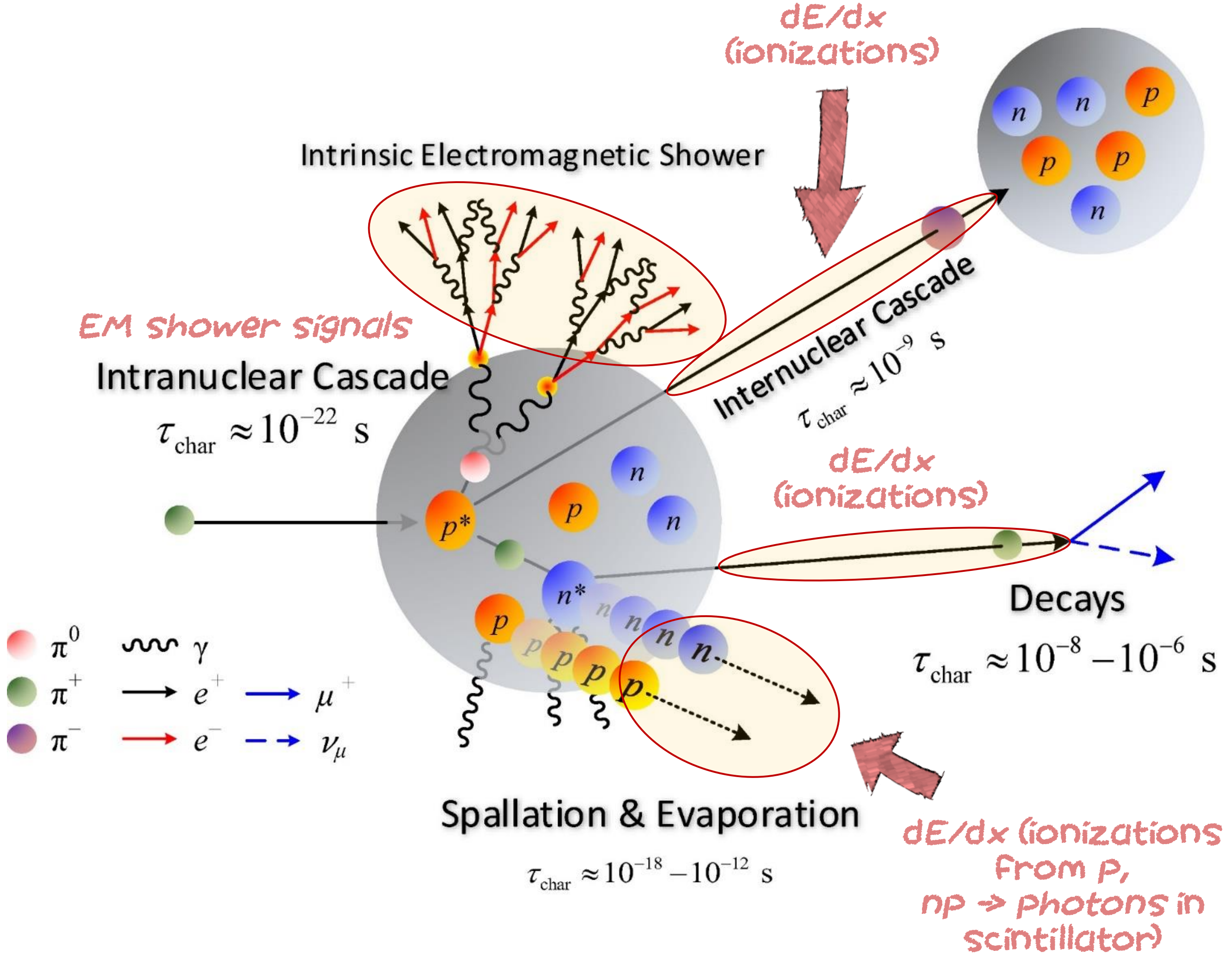

Hadronic Showers

GEANT4 Simulation: 10 GeV π^+ in copper

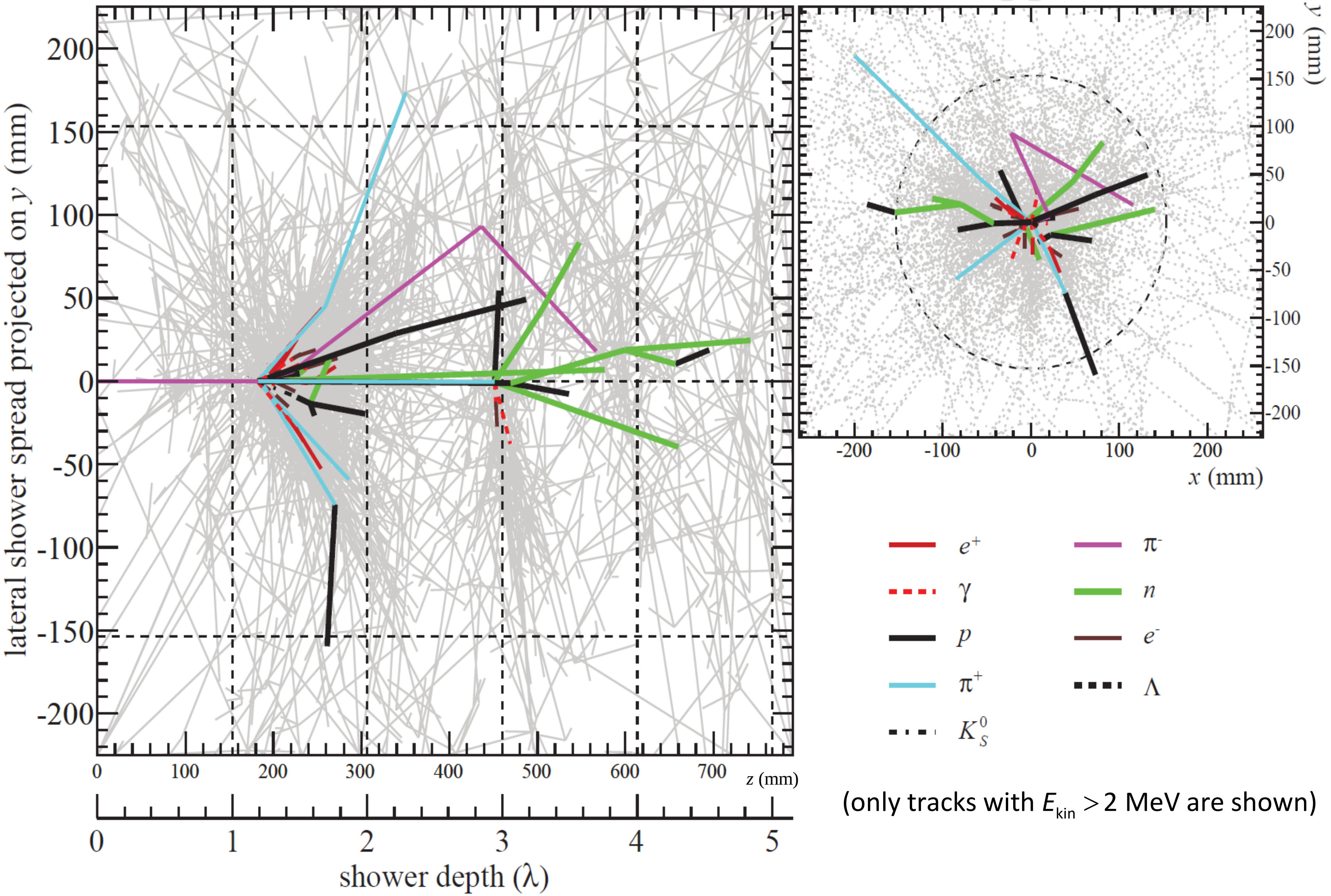

(only tracks with $E_{kin} > 2$ MeV are shown)

Hadronic Showers

GEANT4 Simulation: 10 GeV π^+ in copper

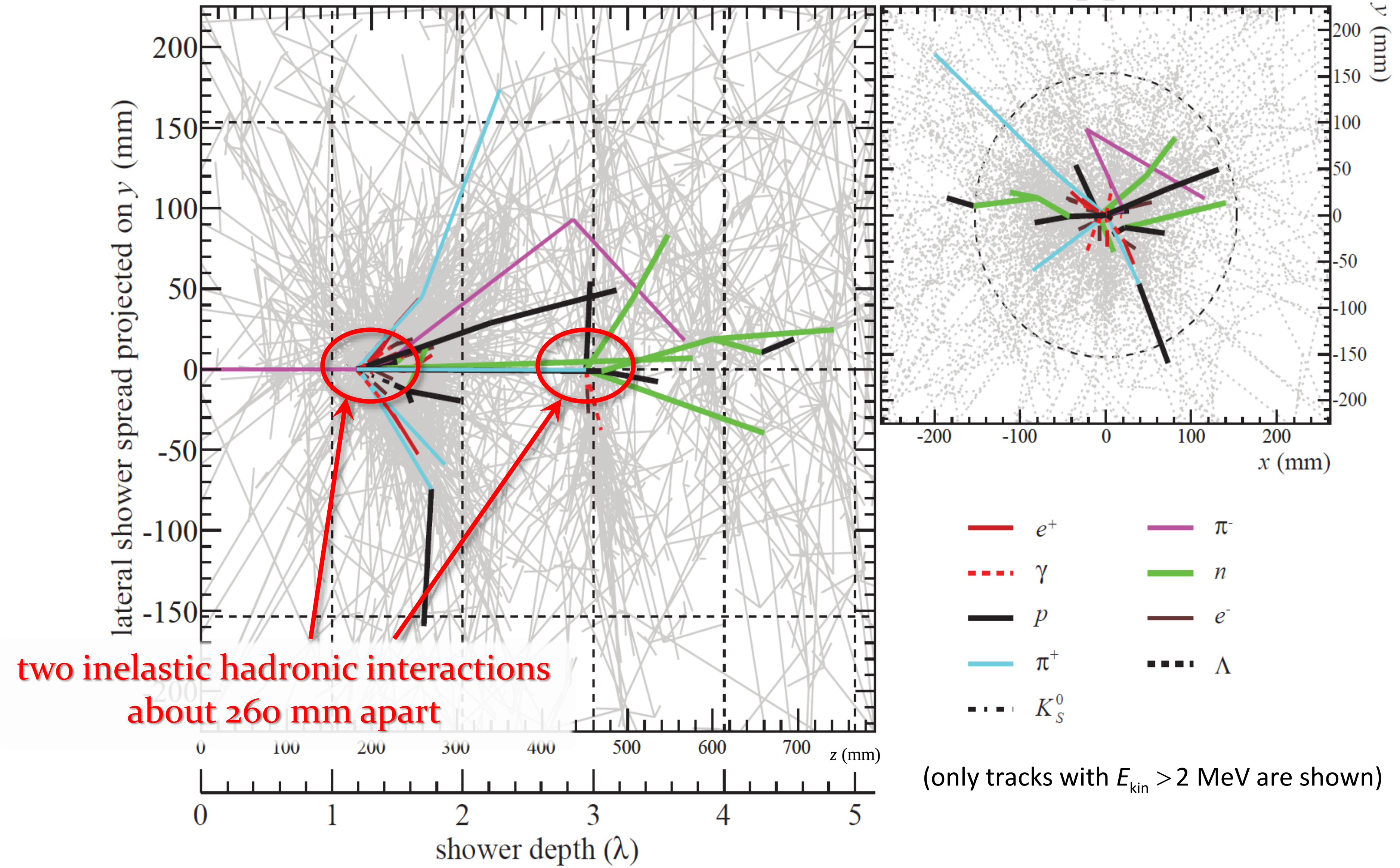

(only tracks with $E_{kin} > 2$ MeV are shown)

Hadronic Showers

GEANT4 Simulation: 10 GeV π^+ in copper

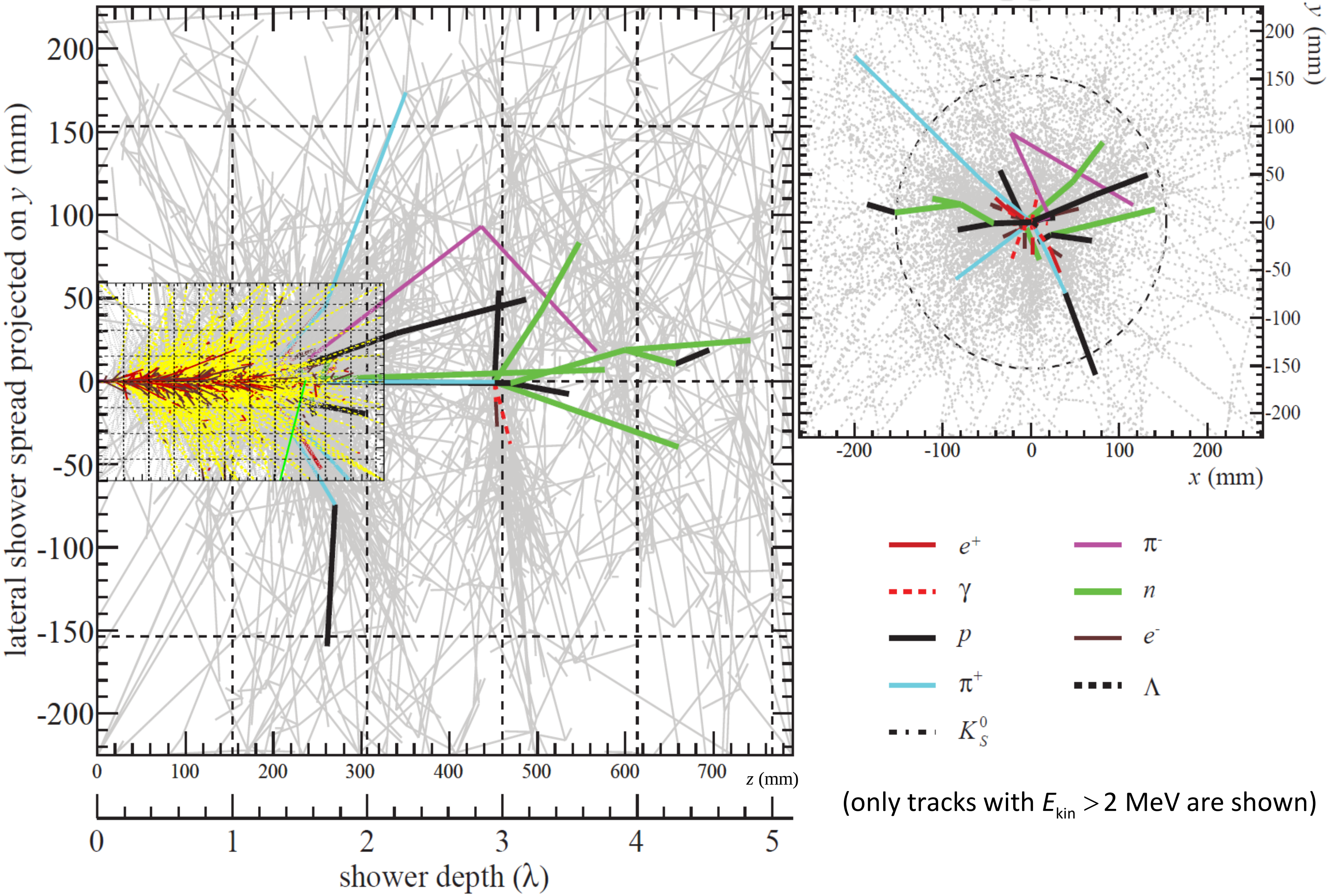

(only tracks with $E_{kin} > 2$ MeV are shown)

Direct comparison of longitudinal profiles

- Absolute energy loss per unit depth in EM and HAD shower in the same calorimeter

Testbeam data

P. Loch (Diss.), University of Hamburg 1992

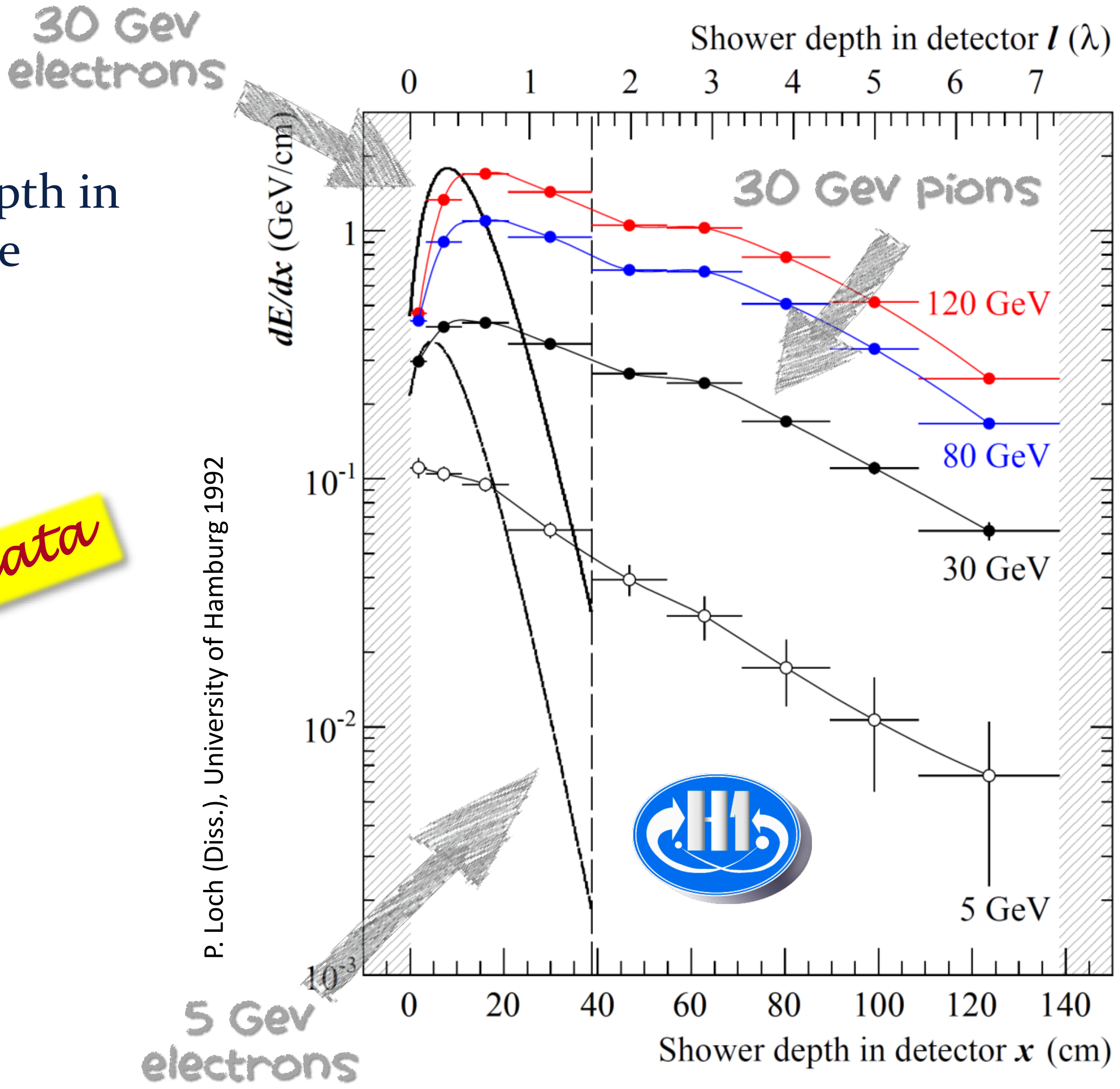

Moving on to the Experiment (1988-1992)

- H1 @ HERA (DESY Hamburg, 1992-2010)
  - Deep inelastic electron/positron-proton scattering –
  - Remove electron signals (in neutral current scattering) defines the hadronic final state in the calorimeter…

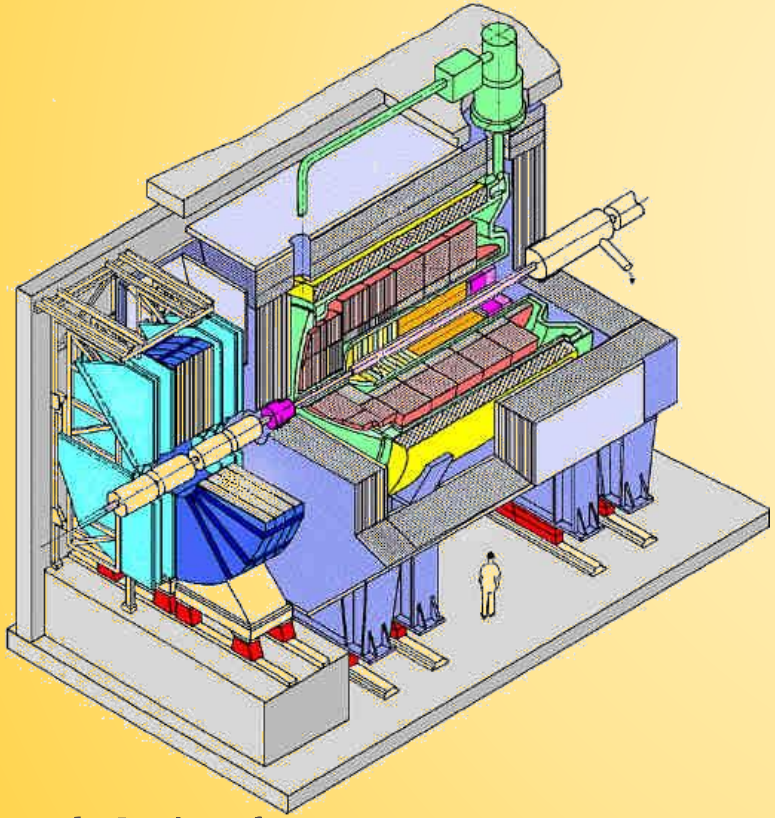

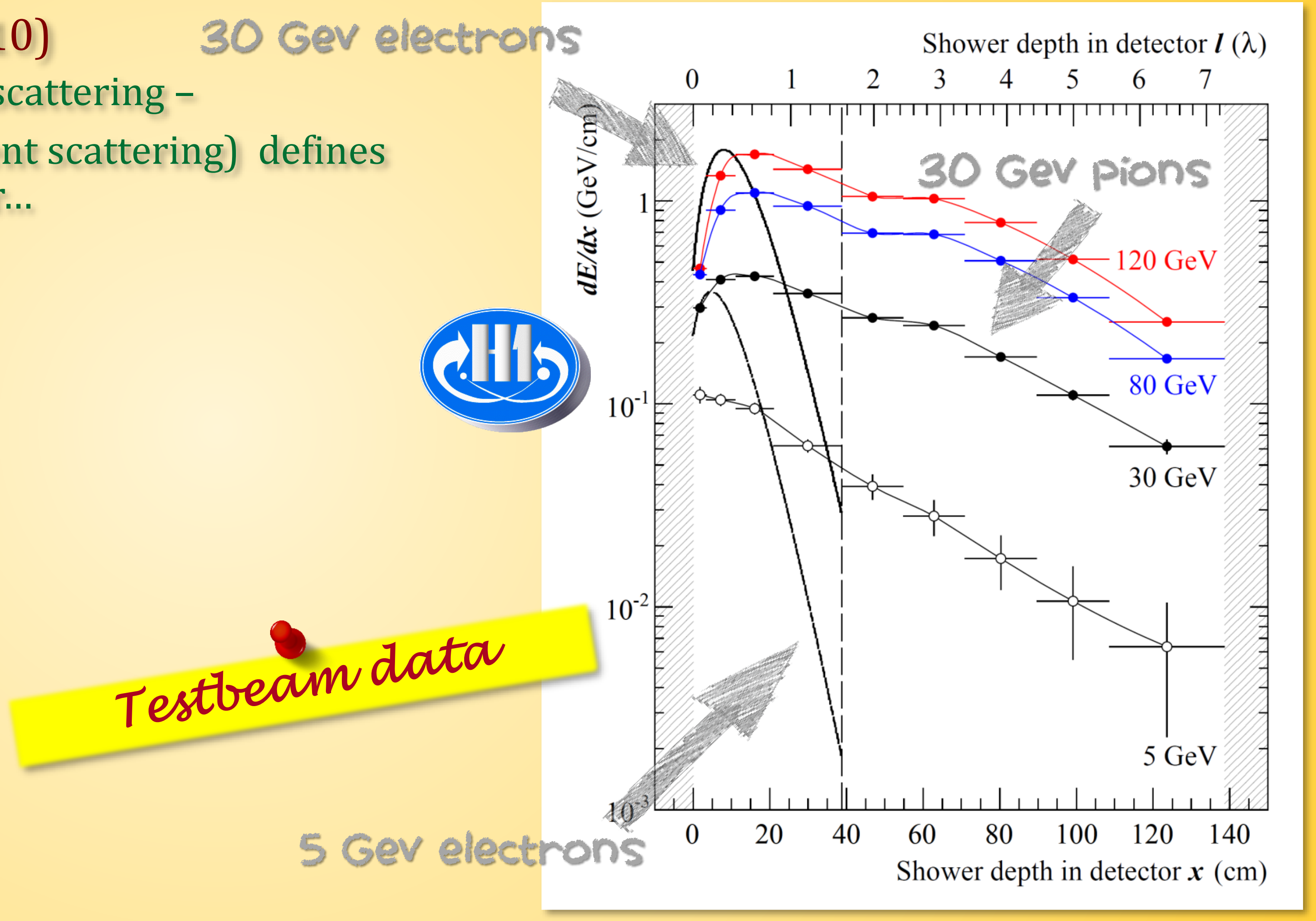

Moving on to the Experiment (1992-1993)

- H1 @ HERA (DESY Hamburg, 1992-2010)
  - Deep inelastic electron/positron-proton scattering –
  - Remove electron signals (in neutral current scattering) defines the hadronic final state in the calorimeter…
- GEM at SSC (defunct)
  - A zoo for calorimeters – have an idea, will be implemented (included tens of unbuildable, environmentally and operationally dangerous designs…)
  - Baby-steps for the forward calorimeter now in ATLAS…

Moving on to the Experiment (1993-1995)

- H1 @ HERA (DESY Hamburg, 1992-2010)
  - Deep inelastic electron/positron-proton scattering –
  - Remove electron signals (in neutral current scattering) defines the hadronic final state in the calorimeter…
- GEM at SSC (defunct)
  - A zoo for calorimeters – have an idea, will be implemented (included tens of unbuildable, environmentally and operationally dangerous designs…)
  - Baby-steps for the forward calorimeter now in ATLAS…

Moving on to the Experiment (1995-2025?)

- H1 @ HERA (DESY Hamburg, 1992-2010)
  - Deep inelastic electron/positron-proton scattering –
  - Remove electron signals (in neutral current scattering) defines the hadronic final state in the calorimeter…
- GEM at SSC (defunct)
  - A zoo for calorimeters – have an idea, will be implemented (included tens of unbuildable, environmentally and operationally dangerous designs…)
  - Baby-steps for the forward calorimeter now in ATLAS…
- ATLAS at LHC (still alive – don't listen to Tilman!)
  - Complex hadronic final state with underlying event and pile-up
  - Precision jet measurements

CALORIMETERS IN ATLAS

MODULES, READOUT & SIGNAL PROCESSING

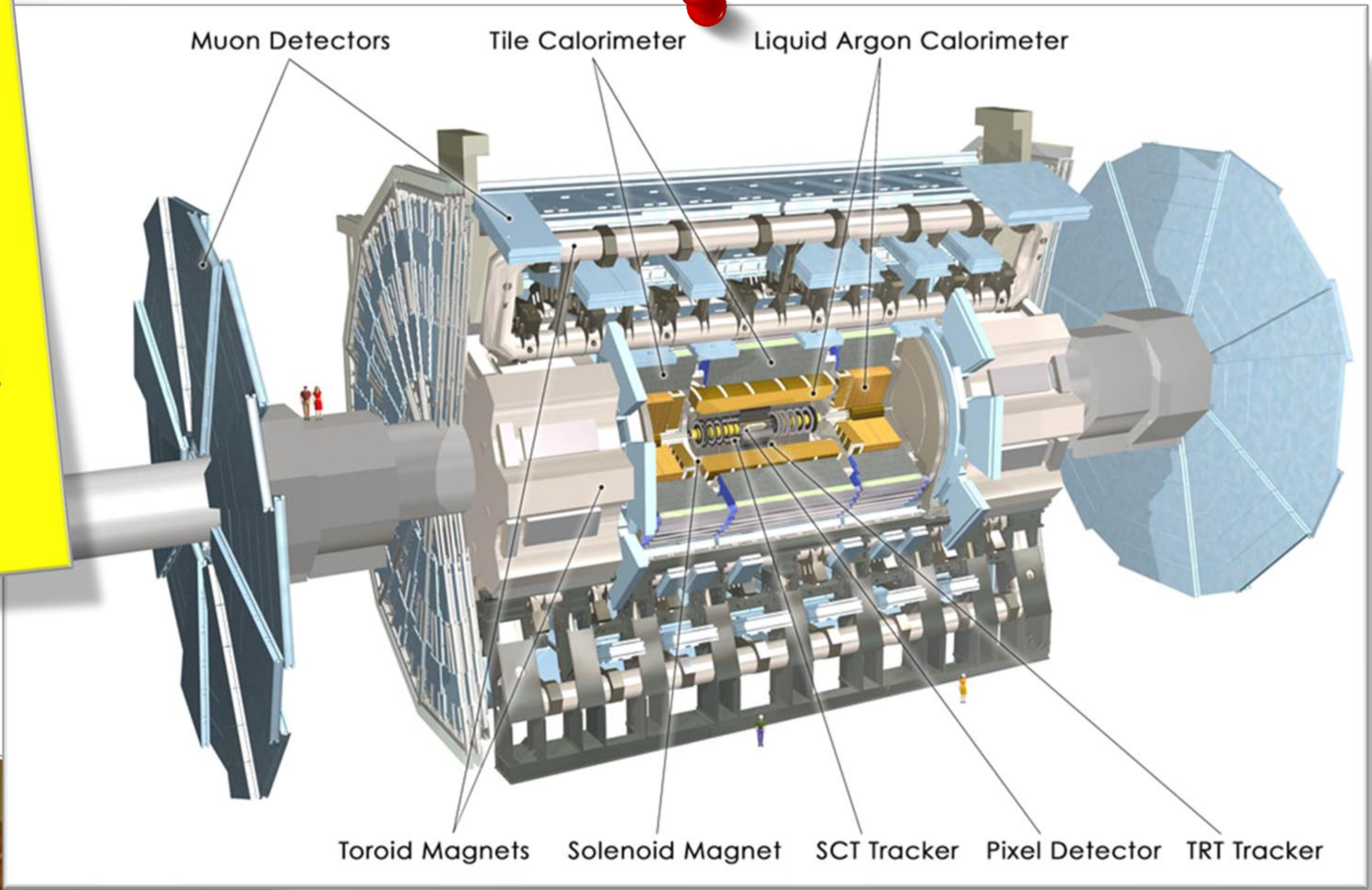

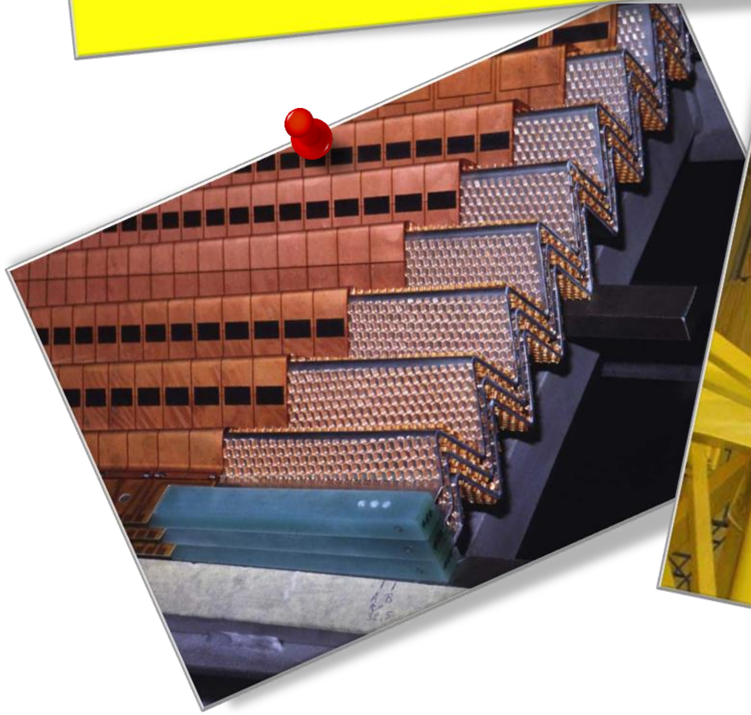

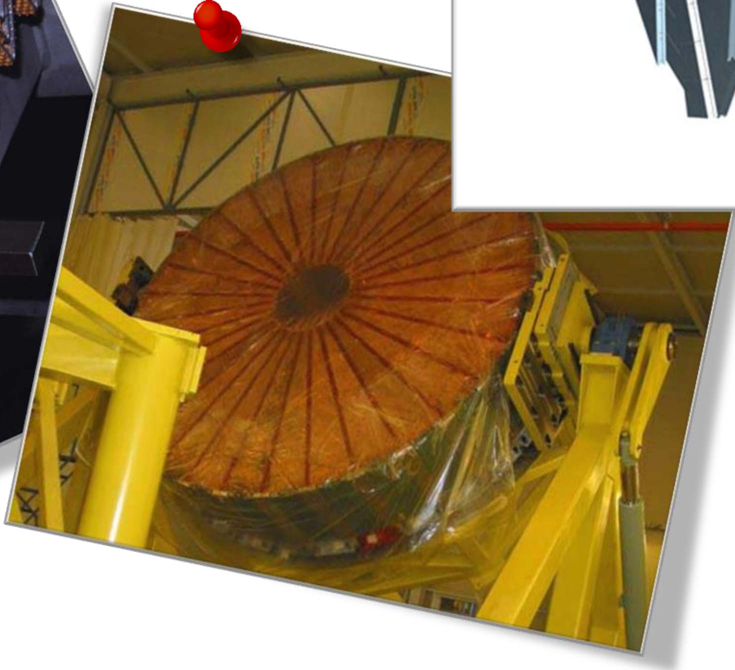

ATLAS Calorimeters

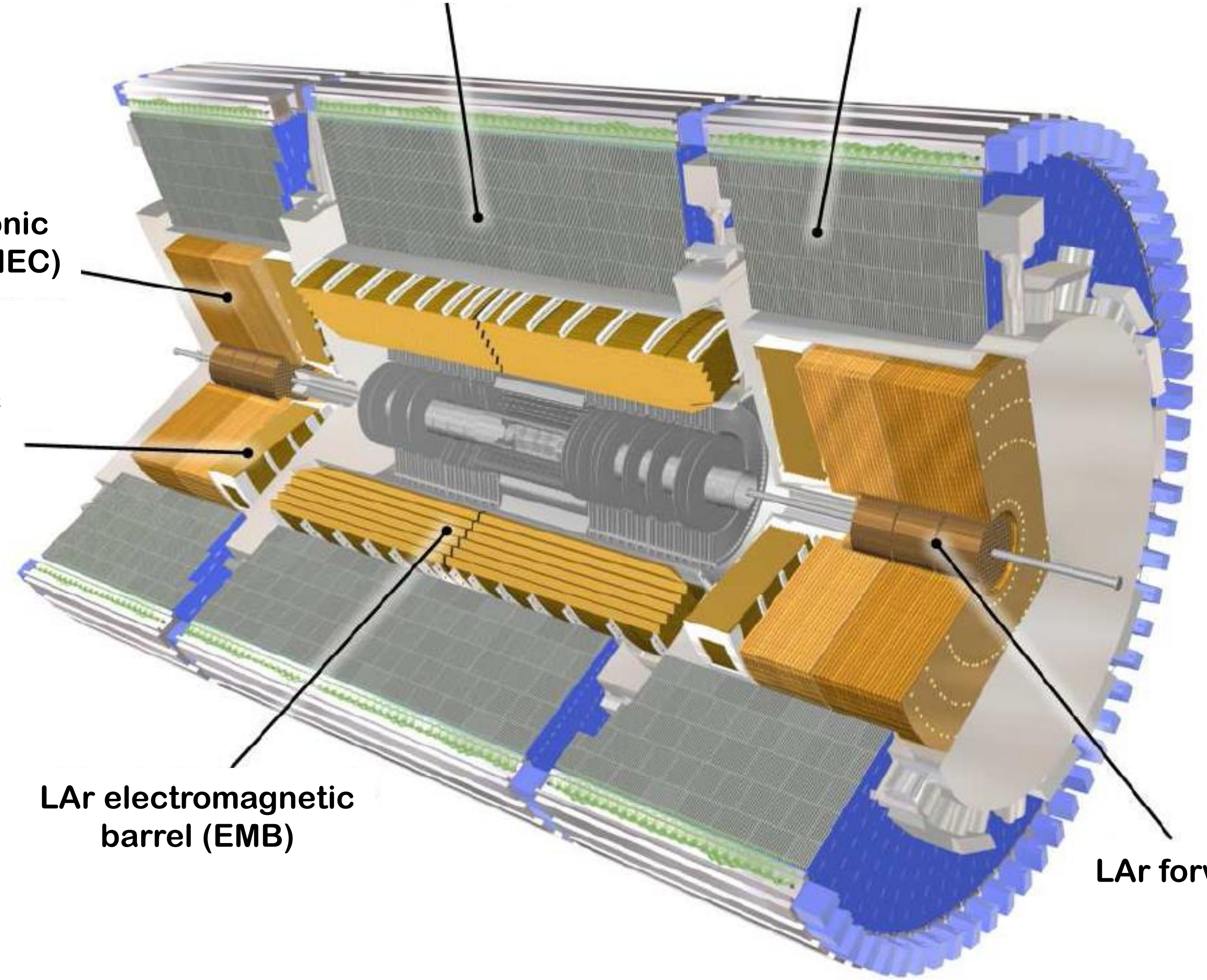

Highly granular EM calorimeters

Liquid argon/lead sampling calorimeter

- No azimuthal discontinuities due to accordion absorber structure in EMB and *Spanish-fan-shaped absorber* in the EMEC
- Up to three longitudinal samplings + pre-sampler*
- Stable operations even in high luminosity running – little to no detector degradation due to ionization rates
- Projective readout cells

Operational considerations

- Slow signal collection in liquid argon (charge collection time $t_d \approx 450$ ns) in the presence of high pile-up (bunch crossings every 25 ns) – bipolar signal shaping

Absorption power

- $24 - 27\ X_0$ for electrons and photons

EMB		109 568	$\|\eta\| < 1.52$	
	PreSamplerB	7 808	$\|\eta\| < 1.52$	$0.025 \times \pi/32$
	EMB1		$\|\eta\| < 1.4$	$0.025/8 \times \pi/32$
			$1.4 < \|\eta\| < 1.475$	$0.025 \times \pi/128$
	EMB2		$\|\eta\| < 1.4$	$0.025 \times \pi/128$
			$1.4 < \|\eta\| < 1.475$	$0.075 \times \pi/128$
	EMB3		$\|\eta\| < 1.35$	$0.050 \times \pi/128$
EMEC		63 744	$1.375 < \|\eta\| < 3.2$	
	PreSamplerE	1 536	$1.5 < \|\eta\| < 1.8$	$0.025 \times \pi/32$
	EME1		$1.375 < \|\eta\| < 1.425$	$0.050 \times \pi/32$
			$1.425 < \|\eta\| < 1.5$	$0.025 \times \pi/32$
			$1.5 < \|\eta\| < 1.8$	$0.025/8 \times \pi/32$
			$1.8 < \|\eta\| < 2.0$	$0.025/6 \times \pi/32$
			$2.0 < \|\eta\| < 2.4$	$0.025/4 \times \pi/32$
			$2.4 < \|\eta\| < 2.5$	$0.025 \times \pi/32$
			$2.5 < \|\eta\| < 3.2$	$0.1 \times \pi/32$
	EME2		$1.375 < \|\eta\| < 1.425$	$0.050 \times \pi/128$
			$1.425 < \|\eta\| < 2.5$	$0.025 \times \pi/128$
			$2.5 < \|\eta\| < 3.2$	$0.1 \times \pi/128$
	EME3		$1.5 < \|\eta\| < 2.5$	$0.050 \times \pi/128$

3 longitudinal segments in $|\eta| < 1.52$ (EMB1-3)

3 longitudinal segments in $1.375 < |\eta| < 2.5$ (EME1-3), 2 longitudinal segments in $2.5 < |\eta| < 3.2$ (EME1-2)

173,312 independent readout channelss

*readout layer ("massless gap") between cryostat wall and front face of calorimeter – provides signal proportional to energy loss in upstream material

Electromagnetic Calorimeters in ATLAS

EMB material budget

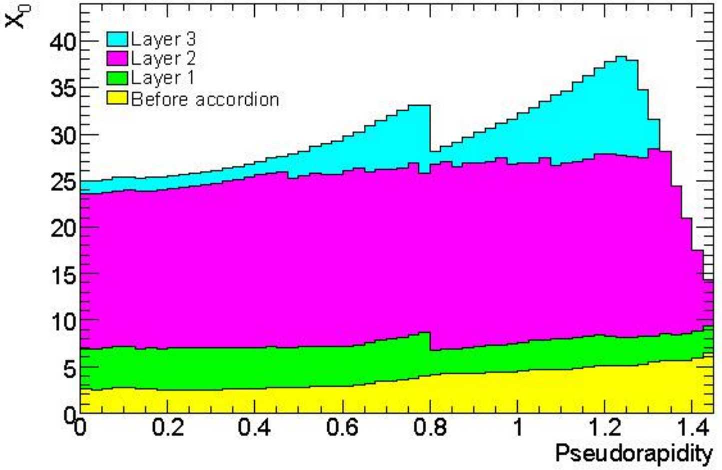

EMEC material budget

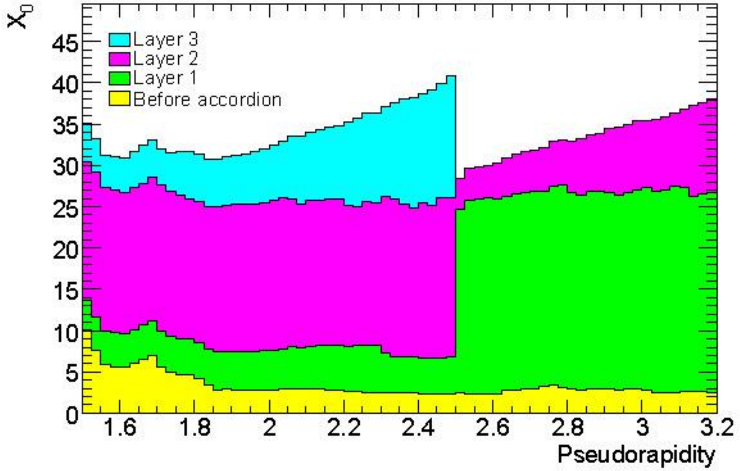

EMB readout segment

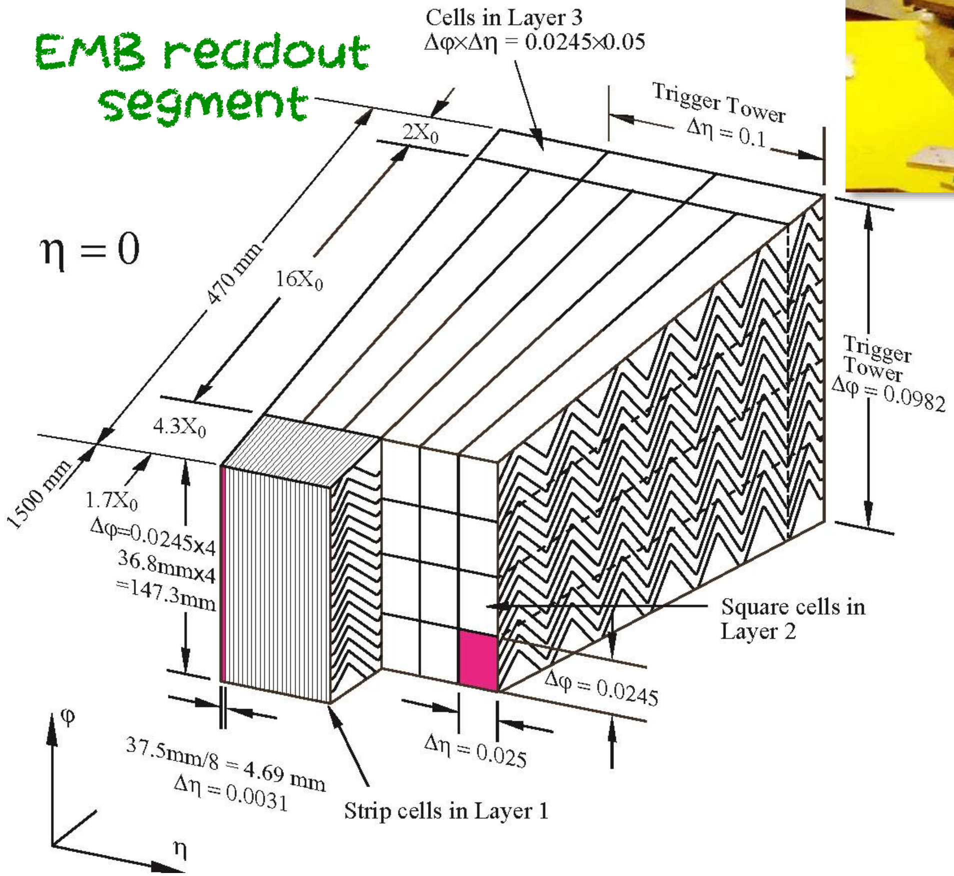

EMEC module construction ~1/4 of wheel assembled

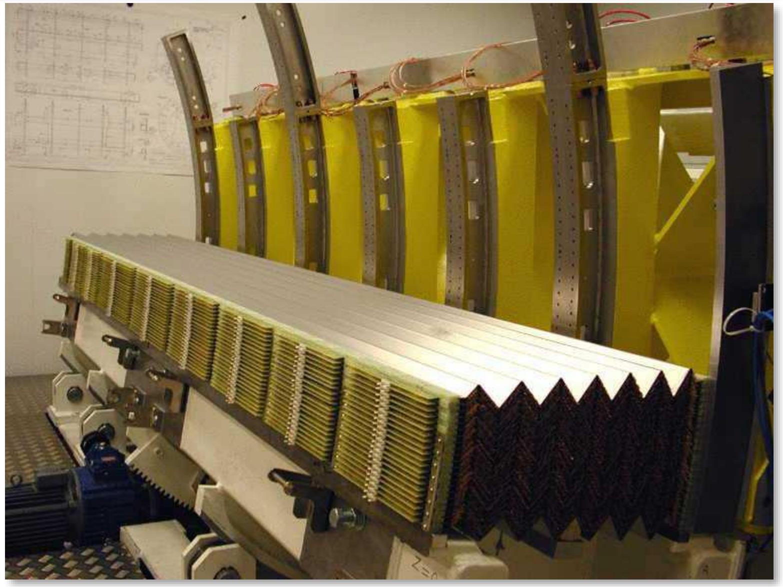

EMB absorber stacking

Hadronic Calorimeters in ATLAS

Central hadronic calorimeters

- Scintillator/steel tile calorimeter
  - Signal is carried by photons and collected by photomultiplier tubes (2 channels per cell)
  - Three longitudinal samplings with a projective readout geometry
  - Fast signal within 50 ns – reduced effect of pile-up on signal, (near) unipolar signals

End-cap hadronic calorimeter

- Liquid argon/copper calorimeter
  - Four longitudinal samples
  - High stability in signal generation without observable detector degradation due to high luminosities
  - Projective readout geometry

Forward calorimeter

- Liquid argon/copper (EM) and liquid argon/tungsten (HAD)
  - Thin gap calorimeter (charge collection time $t_d \approx 50$ ns) optimized for high ionization rates due to pile-up
  - Non-projective readout geometry features electrodes parallel to beam line
  - Dense absorber acts as radiation shield for muon spectrometer

Hadronic calorimeters	Tile (barrel)	2 880	$\|\eta\| < 1$	
	TileBar0/1			$0.1 \times \pi/32$
	TileBar2			$0.2 \times \pi/32$
	Tile (extended barrel)	2 304	$0.8 < \|\eta\| < 1.7$	
	TileExt0/1			$0.1 \times \pi/32$
	TileExt2			$0.2 \times \pi/32$
	HEC	5 632	$1.5 < \|\eta\| < 3.2$	
	HEC0/1/2/3		$1.5 < \|\eta\| < 2.5$	$0.1 \times \pi/32$
			$2.5 < \|\eta\| < 3.2$	$0.2 \times \pi/16$
Forward calorimeters	FCAL	3 524	$3.1 < \|\eta\| < 4.9$	$\Delta x \times \Delta y$
	FCAL0		$3.1 < \|\eta\| < 3.15$	1.5 cm × 1.3 cm
			$3.15 < \|\eta\| < 4.3$	3.0 cm × 2.6 cm
			$4.3 < \|\eta\| < 4.83$	1.5 cm × 1.3 cm
	FCAL1		$3.2 < \|\eta\| < 3.24$	1.7 cm × 2.1 cm
			$3.24 < \|\eta\| < 4.5$	3.3 cm × 4.2 cm
			$4.5 < \|\eta\| < 4.81$	1.7 cm × 2.1 cm
	FCAL2		$3.29 < \|\eta\| < 3.32$	2.7 cm × 2.4 cm
			$3.32 < \|\eta\| < 4.6$	5.4 cm × 4.7 cm
			$4.6 < \|\eta\| < 4.75$	2.7 cm × 2.4 cm

14,340 individual channels in total*

Full hadronic coverage provided by the EM and HAD calorimeters with a combined depth $\geq 10\lambda$ nearly everywhere within the whole acceptance $|\eta| \lesssim 4.9$

Calorimeter readout

177,540	regular calorimeter cells
10,112	pre-sampler/gap scintillator
187,652	independent readout channels

*Tile has dual readout (2 electronic channels per cell) with only one of those used for cell energy measurements

Hadronic Calorimeters in ATLAS

Hadronic depth along rapidity

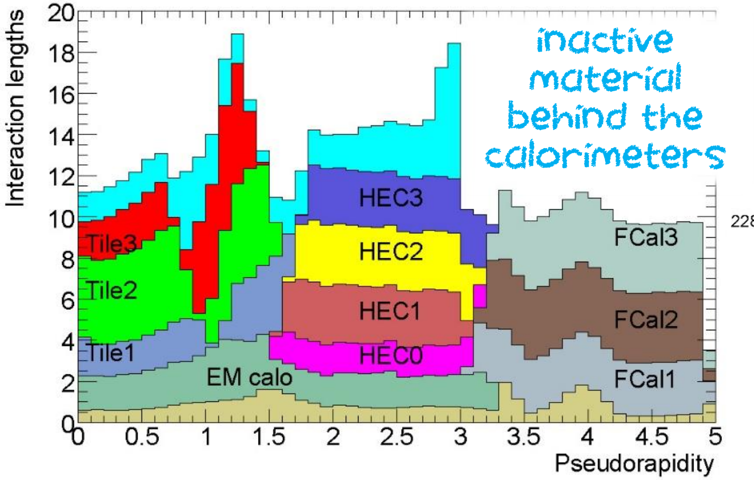

inactive material behind the calorimeters

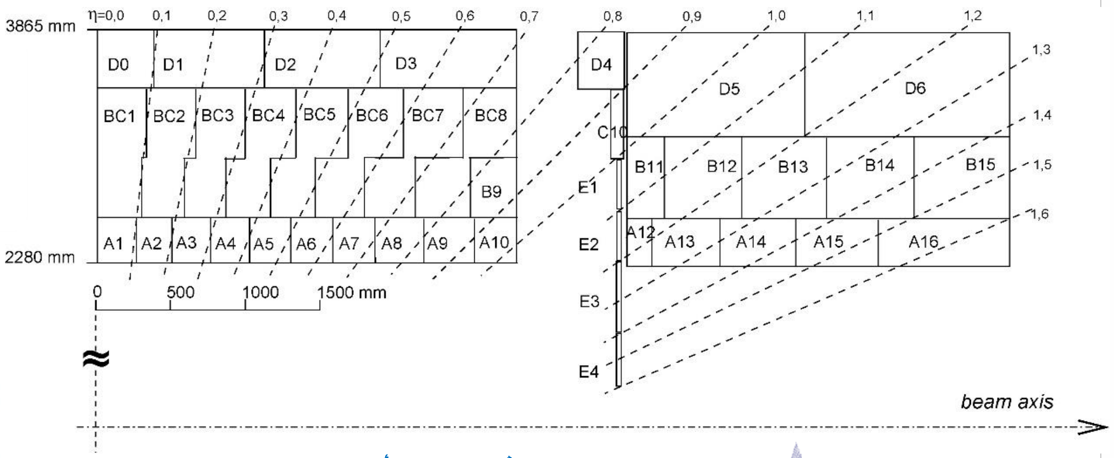

Tile readout geometry

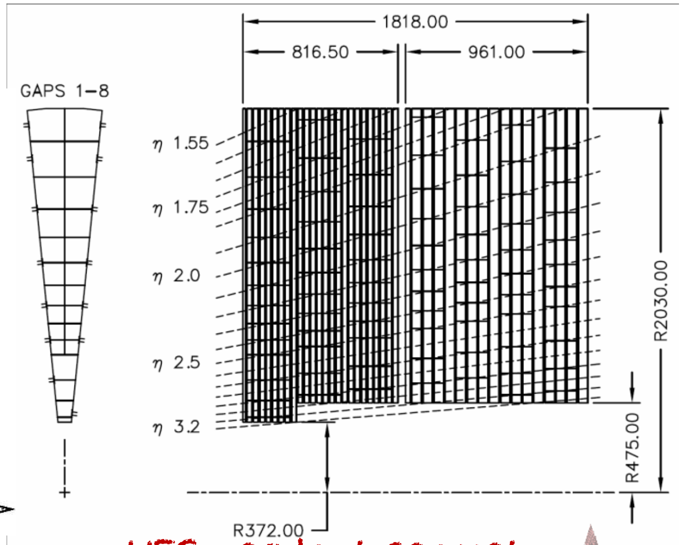

HEC readout geometry

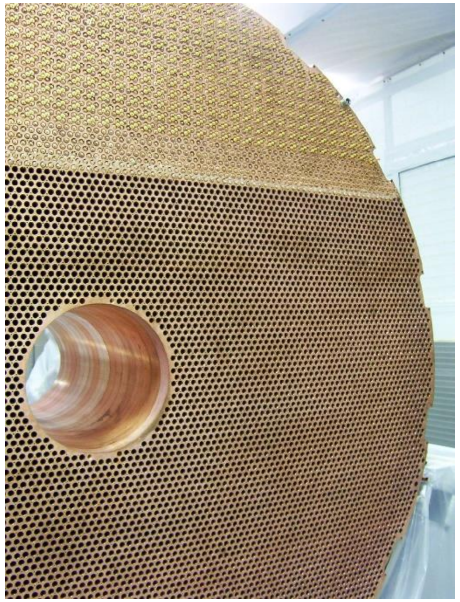

FCal 2/3 electrodes with tungsten form pieces

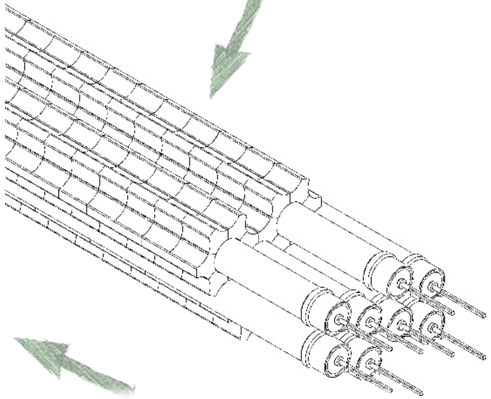

FCal 1 module partly instrumented

Tile segment

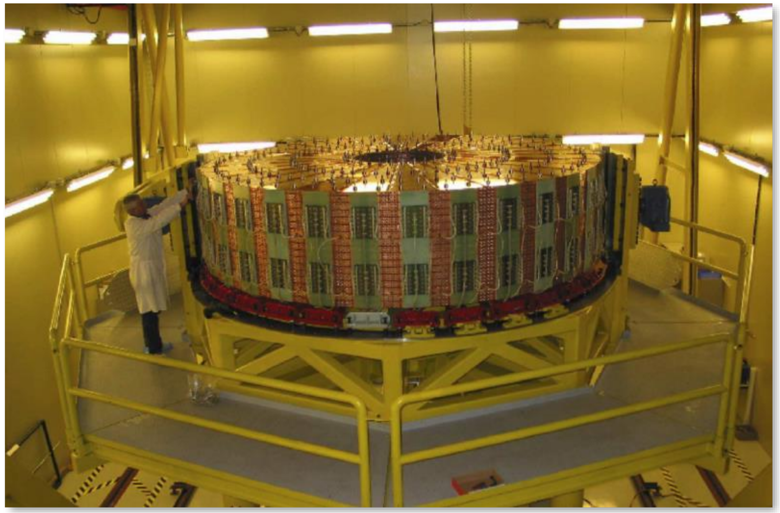

HEC complete wheel

Signal Formation Example: ATLAS LAr Calorimeter

Sampling calorimeter

Ionization electrons collected in electric field between absorbers

- Collect charge in electric field E
- Measure current

Characteristic features

Collected charge and current are proportional to energy deposited in active medium

- $Q(t = t_d) = N_e e/2$
- $I(t = t_0) = N_e e/t_d$
- $N_e(t) = N_e(t = t_0)/d \cdot (d - x(t))$

Drift time t_d for electrons in active medium

- Determines charge collection time
- Can be adjusted to optimize calorimeter performance
- $t_d \approx 450(50)$ ns for $d = 2.25(0.25)$ mm and $E = 1$ kV/mm field – values in () are for the FCal

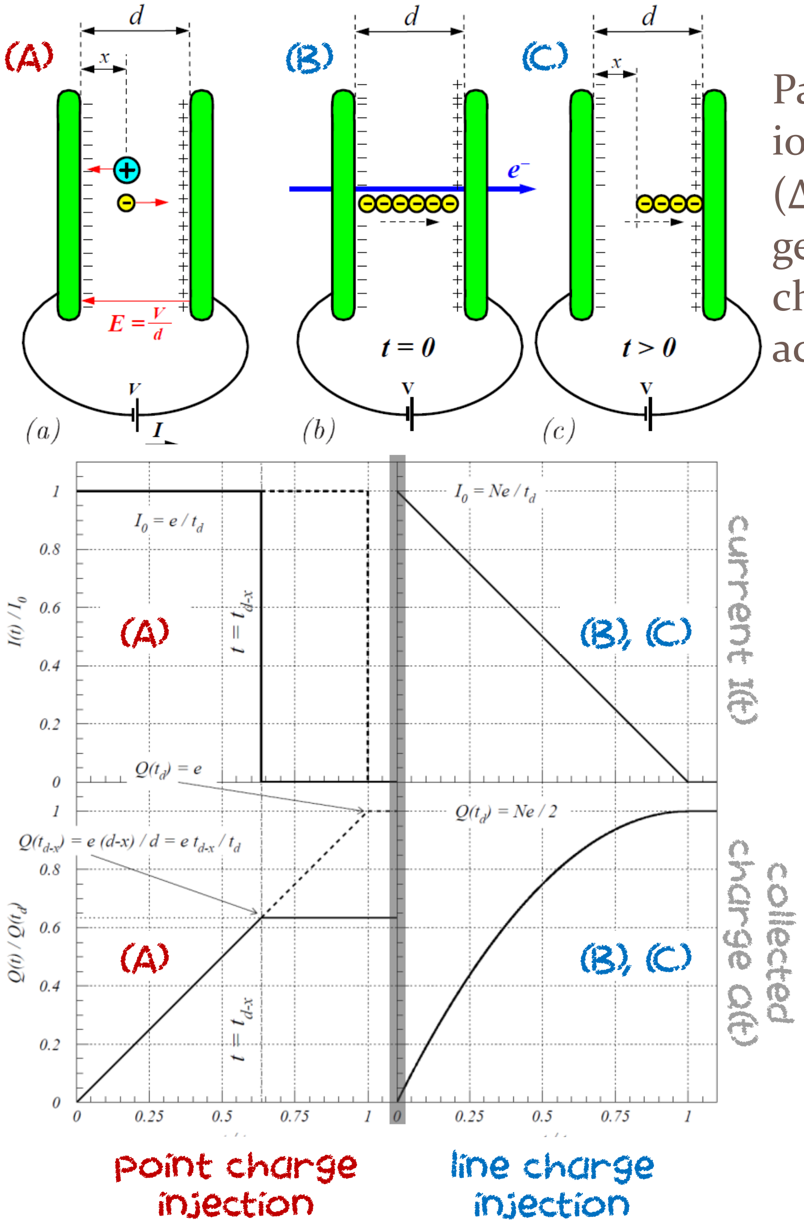

Passage of fast ionizing particle ($\Delta t_{x=0}^{x=d} \ll t_d$) generates line charge in the active medium

$$I_0 = \frac{Q = N \times e}{t_d} \propto E_0$$

$$Q(t_d) = \frac{N \times e}{2} \propto E_0$$

ATLAS LAr Calorimeter: From Signal to Cell Energy Response

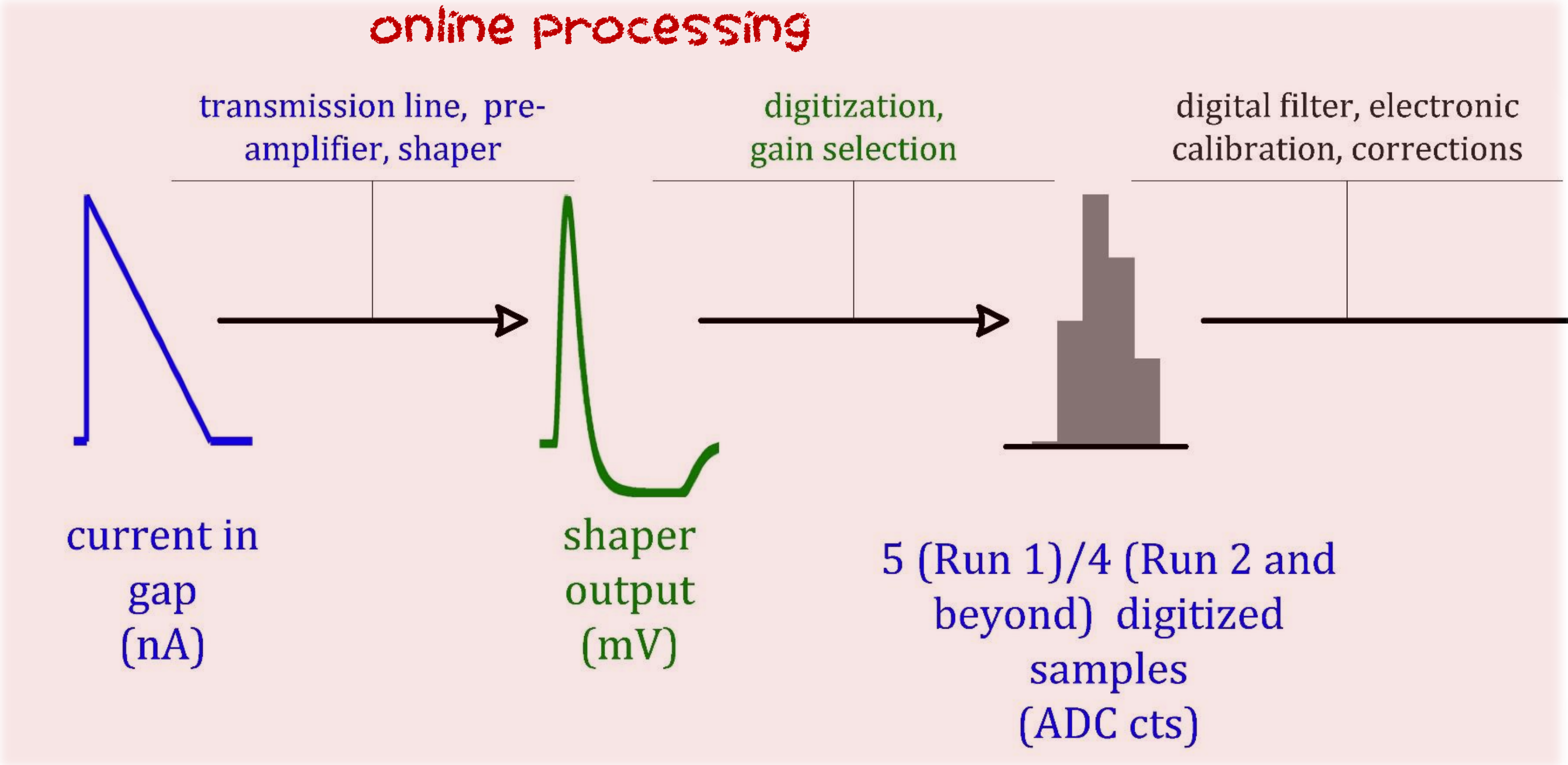

same information content for LAr and Tile cells!

Cell Data

- energy E_{raw} (MeV)
- time t (ns)
- quality Q
- selected gain g
- online id id_{online}
- provenance p

provenance: flags signal processing (e.g., filtered reconstruction) masked cells (e.g., noise bursts), estimated signal for dead cells, etc. ...

$$E_{raw} = A_{peak} \times \underbrace{\underbrace{[\text{bunch intensity}]}_{\text{correction for position of bunch crossing in train}} \times \underbrace{[\text{ADC} \rightarrow \text{nA}]}_{\text{current calibration}}}_{\text{online}}$$

$$\times \underbrace{([\text{HV}] \times [\text{cross-talk}] \times [\text{purity}])}_{\text{electronic and efficiency corrections}} \times \underbrace{[\text{nA} \rightarrow \text{MeV}]}_{\text{energy calibration}}$$

Cell signal at electromagnetic energy scale

ATLAS EXPERIMENT

What is response?

- Reconstructed calorimeter signal
  - Based on the direct measurement – the raw signal
  - May include noise suppression (digital filtering)
  - All cell level corrections for hardware failures and run conditions are applied
- Has the concept of **signal** (or **energy**) **scale**
  - Basic signal before final calibrations (EM scale)
  - Derived from electron signals in test beams and monitored *in-situ* in collision events
  - Ideal EM scale – does not reconstruct full particle energy!

$$E_{\text{raw}} = \underbrace{A_{\text{peak}} \times \underbrace{[\text{bunch intensity}]}_{\text{correction for position of bunch crossing in train}} \times \underbrace{[\text{ADC} \rightarrow \text{nA}]}_{\text{current calibration}}}_{\text{online}}$$

$$\times \underbrace{([\text{HV}] \times [\text{cross-talk}] \times [\text{purity}])}_{\text{electronic and efficiency corrections}} \times \underbrace{[\text{nA} \rightarrow \text{MeV}]}_{\text{energy calibration}}$$

Same information content for LAr and Tile cells!

Cell Data

- energy E_{raw} **(MeV)**
- time t **(ns)**
- quality Q
- selected gain g
- online id id_{online}
- provenance p

Provenance: flags signal processing (e.g., filtered reconstruction) masked cells (e.g., noise bursts), estimated signal for dead cells, etc. ...

Cell signal at electromagnetic energy scale

Pile-up in the ATLAS LAr Calorimeter

Pile-up at the LHC

Origin

High collision luminosity = proton beam intensities ⊗ bunch crossing frequency ⊗ high inclusive *pp* cross section

Comparably slow signal collection in LAr

In-time pile-up

Signals generated by particles from additional *pp* collisions in the same bunch crossing

Out-of-time pile-up

Signal fragments from previous and following bunch crossing added to the in-time signal

Online mitigation strategy

Fast bipolar signal shaping measures current $I_0 = I(t = 0)$

Shape has integral zero – in-time pile-up is on average canceled by out-of-time pile-up due to negative weight of signal remnants

Prog.Part.Nucl.Phys.60:484-551,2008

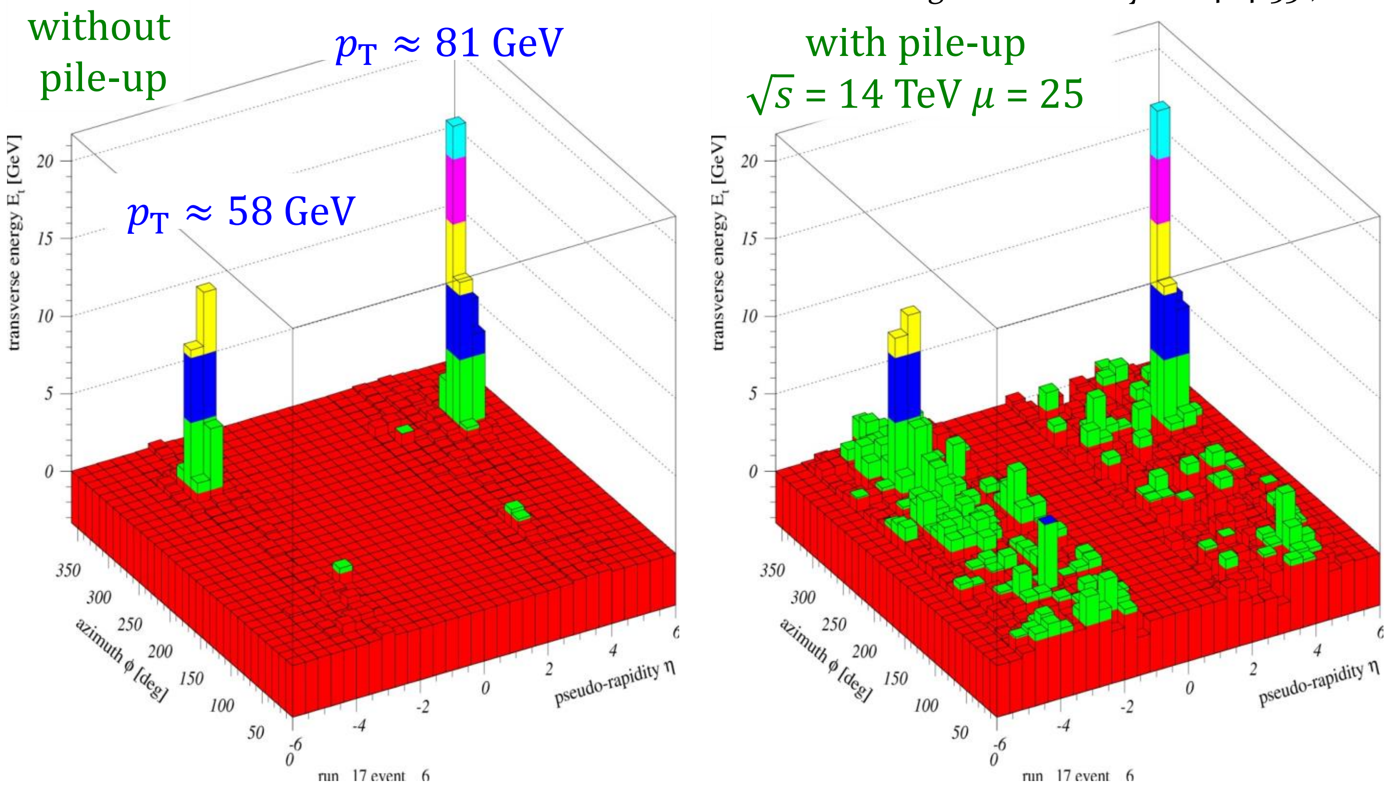

Pile-up in the ATLAS LAr Calorimeter

Pile-up at the LHC

Origin

High collision luminosity = proton beam intensities ⊗ bunch crossing frequency ⊗ high inclusive *pp* cross section

Comparably slow signal collection in LAr

In-time pile-up

Signals generated by particles from additional *pp* collisions in the same bunch crossing

Out-of-time pile-up

Signal fragments from previous and following bunch crossing added to the in-time signal

Online mitigation strategy

Fast bipolar signal shaping measures current $I_0 = I(t = 0)$

Shape has integral zero – in-time pile-up is on average canceled by out-of-time pile-up due to negative weight of signal remnants

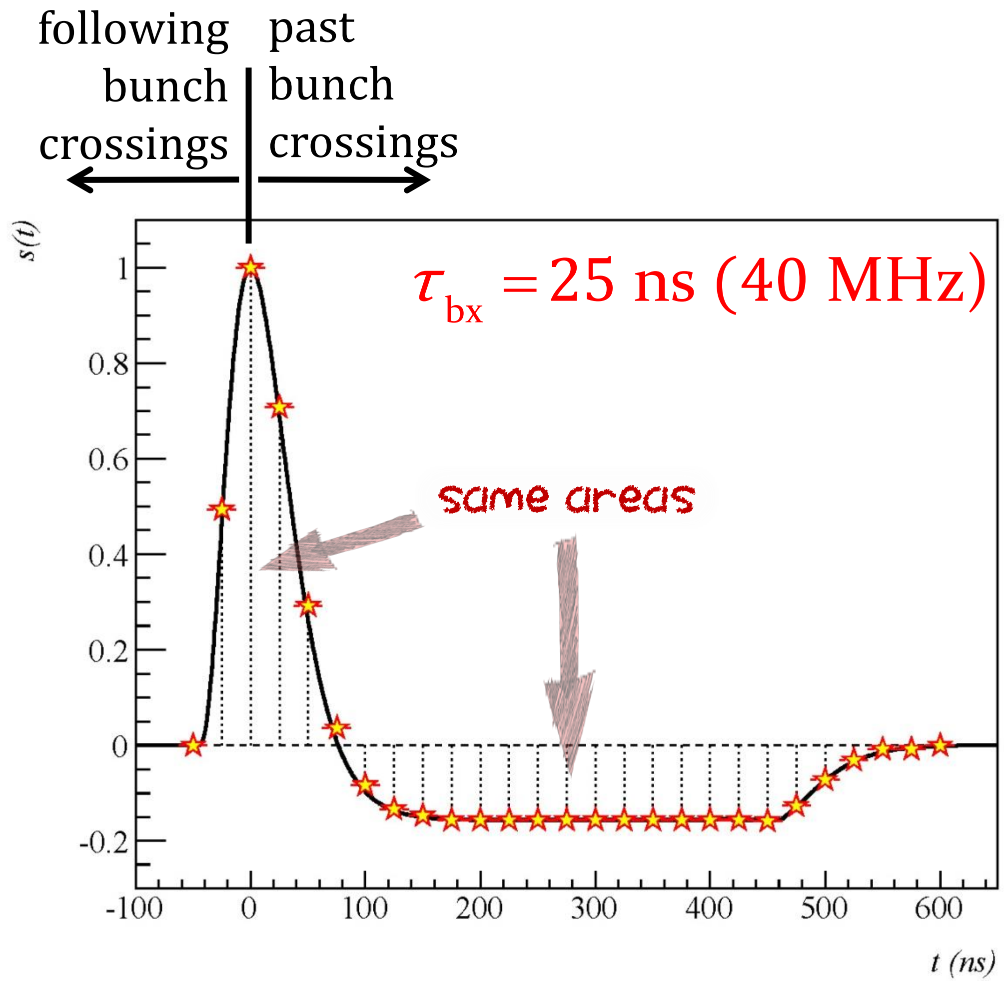

Digital Signal Filter

Concept

W.E. Cleland and E.G. Stern, Nucl. Inst. Meth. **A338 (1994) 467.**

- Unfold physics pulse shape from a measured pulse shape
  - Pulse shape measured in 4 digital samples s_i taken at $t_0 + 25$ ns, t_0, $t_0 - 25$ ns, $t_0 - 50$ ns
  - Measured (digitized) shape is affected by transmission line characteristics and signal transfer functions introduces by e.g., impedance mismatches in the readout electronics
  - Linear filter with coefficients a_i constraint by pulse shape –
    - $\sum_{i=1}^{N_s} a_i g_i = 1$
  - g_i is normalized pulse shape in sample i at time t_i, with
    - $\sum_{i=1}^{N_s} a_i \, \partial g_i / \partial t = 0$
- Digital filtering
  - Amplitude/peak $\propto I_0 \propto E_0$
    - $A_{\text{peak}} = \sum_{i=1}^{N_s} a_i (s_i - p_i)$
  - with the sample reading s_i and the pedestal reading p_i (ADC counts for $I = 0$ on input to electronics)
  - Peak time:
    - $A_{\text{peak}} t_{\text{peak}} = \sum_{i=1}^{N_s} b_i (s_i - p_i)$
- Calibration system
  - Coefficients – constraint by injecting known current pulses in the electronic chain and transfer observed calibrated pulse shape to known physics pulse shapes
  - Pedestals – read samples without injecting current into the system and measure average and fluctuations (electronic noise)
  - Auto-correlation – signal history couples fluctuations (noise) in time sampled reading

Formal Extraction of Filter Coefficients

Filter Coefficients

a_i .... digital filter coefficient

R_{ij} .... noise auto-correlation

g_i .... normalized physics pulse shape:

Determined by:
Known pulse shape
Minimizing noise

to 1st order independent of time jitter!

$$\sum_{i=1}^{N_s} a_i g_i = 1$$

$$\sum_{i=1}^{N_s} a_i \frac{\partial g_i}{\partial t} = \sum_{i=1}^{N_s} a_i g_i' = 0$$

$$\sum_{i=1}^{N_s} \sum_{j=1}^{N_s} a_i a_j \sigma_i \sigma_j R_{ij} \rightarrow \min$$

$$a_i = \sum_{j=1}^{N_s} R_{ij}^{-1} \left(\lambda g_j - \mu g_j' \right)$$

$$\lambda = \frac{1}{\Delta} \sum_{i=1}^{N_s} \sum_{j=1}^{N_s} R_{ij}^{-1} g_i' g_j'$$

$$\mu = \frac{1}{\Delta} \sum_{i=1}^{N_s} \sum_{j=1}^{N_s} R_{ij}^{-1} g_i g_j'$$

$$\Delta = \left(\sum_{i=1}^{N_s} \sum_{j=1}^{N_s} R_{ij}^{-1} g_i' g_j' \right) \cdot \left(\sum_{i=1}^{N_s} \sum_{j=1}^{N_s} R_{ij}^{-1} g_i g_j \right) - \left(\sum_{i=1}^{N_s} \sum_{j=1}^{N_s} R_{ij}^{-1} g_i g_j' \right)^2$$

Lagrange Multipliers

CALORIMETER SIGNALS FOR PHYSICS – TOPO-CLUSTER AND TOPO-TOWERS

ATLAS Coll., *Topological cell clustering in the ATLAS calorimeters and its performance in LHC Run 1*
Eur.Phys.J.C.77 (2017) 490
arXiv:1603.02934 [hep-ex]

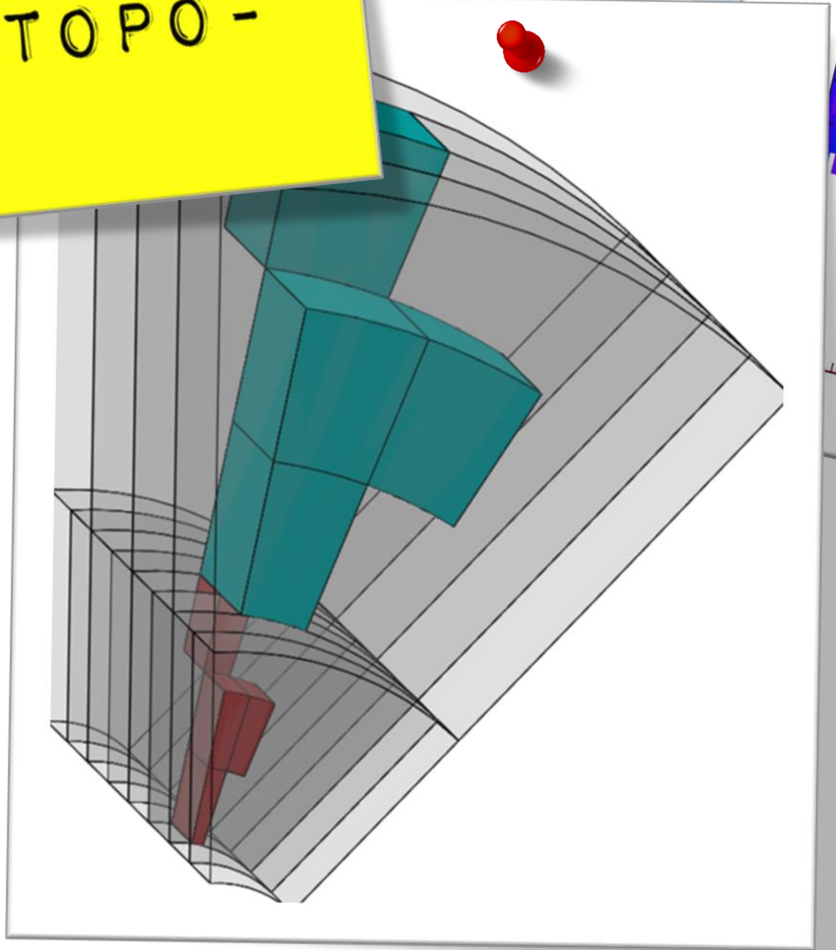

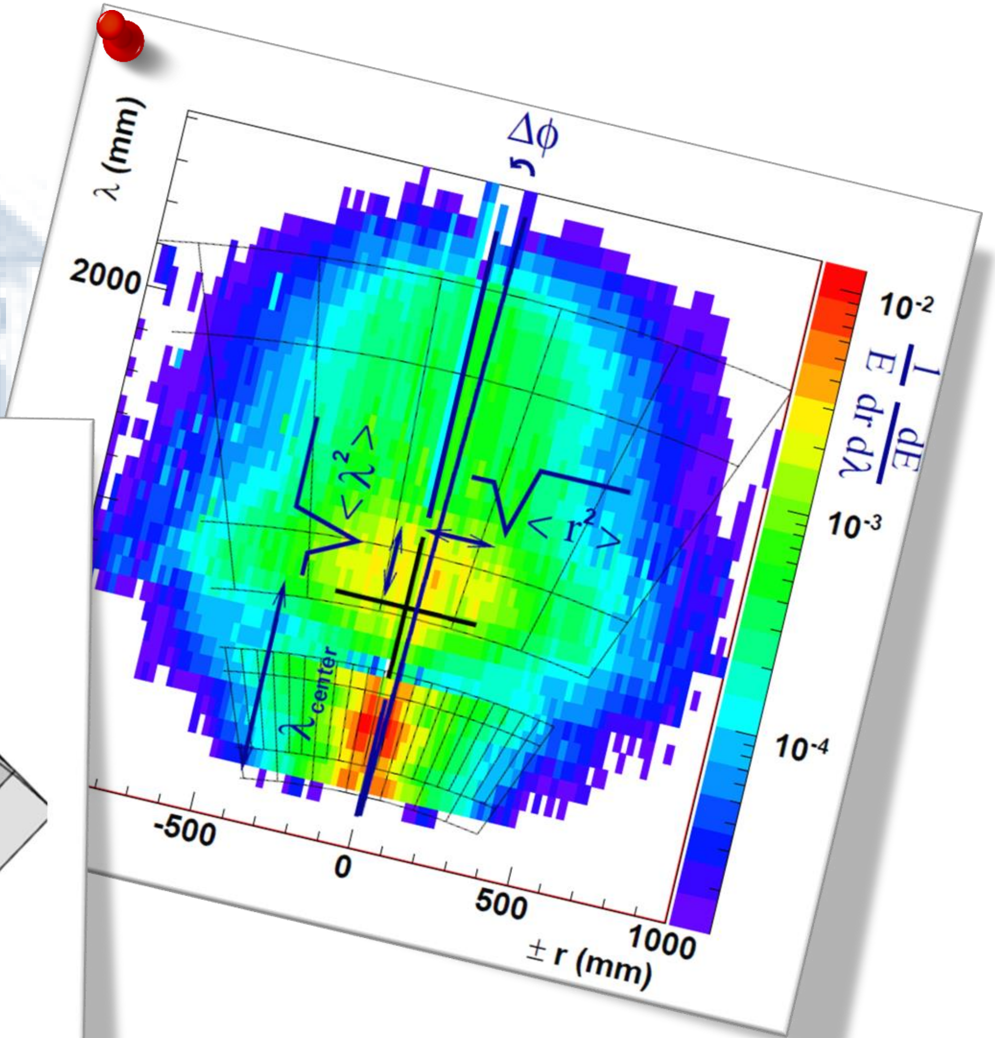

Calorimeter cell signals are collected into topological clusters

- Collects signals from individual or close-by particle showers into 3-dim *energy blobs*
  - Connect cell signals following spatial signal significance patterns in three dimensions
  - Uses seed and growth control conditions, plus envelope
  - Default 4-2-0 configuration ($S = 4$, $N = 2$, $P = 0$)
- Collects cells across subsystem boundaries

$$|E_{\rm cell}^{\rm EM}| > S\,\sigma_{\rm noise,cell}^{\rm EM}$$

$$|E_{\rm cell}^{\rm EM}| > N\sigma_{\rm noise,cell}^{\rm EM}$$

$$|E_{\rm cell}^{\rm EM}| > P\sigma_{\rm noise,cell}^{\rm EM}$$

$$\sigma_{\rm noise} = \begin{cases} \sigma_{\rm noise}^{\rm electronic} & < 2011 \\ \sqrt{\left(\sigma_{\rm noise}^{\rm electronic}\right)^2 + \left(\sigma_{\rm noise}^{\rm pile\text{-}up}\right)^2} & \end{cases}$$

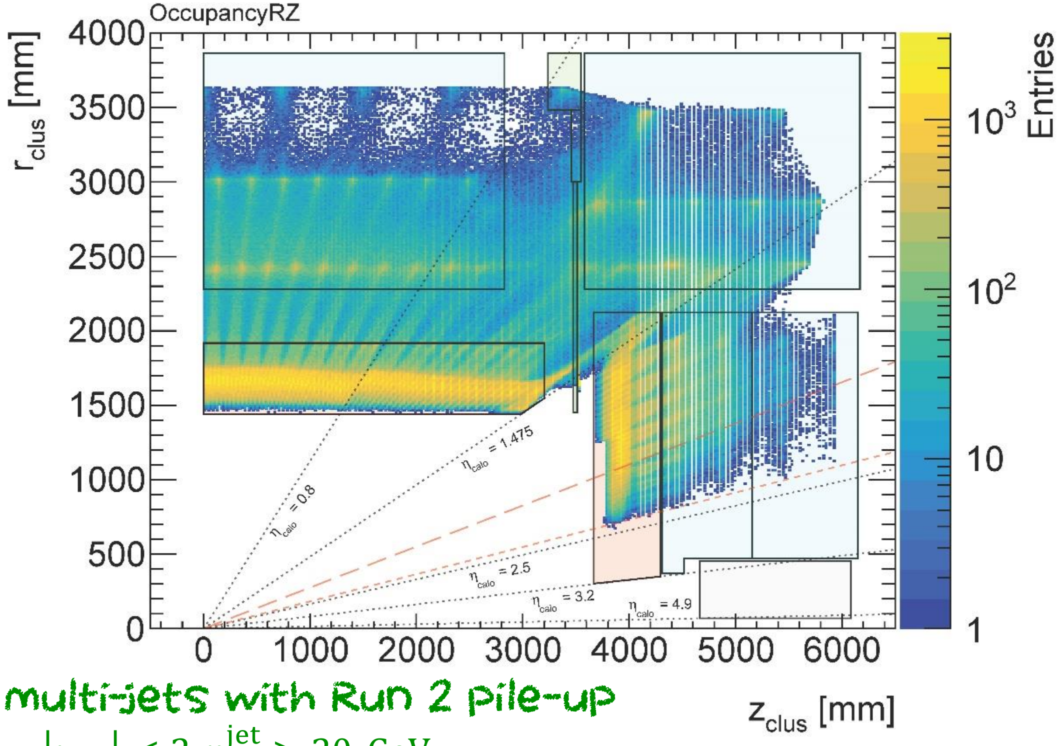

MC16d multi-jets with Run 2 pile-up

$|y_{\rm jet}| < 2, p_{\rm T}^{\rm jet} > 20$ GeV

More on formation

- Growing algorithm requires splitting between local signal maxima
  - Guided by spatial signal structures observed in the high granularity EM calorimeter
  - Splitting efficiency depends on calorimeter readout granularity

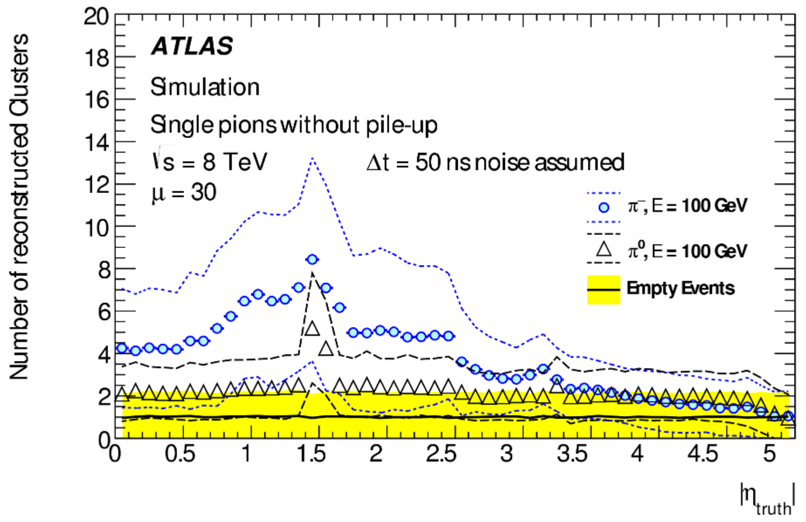

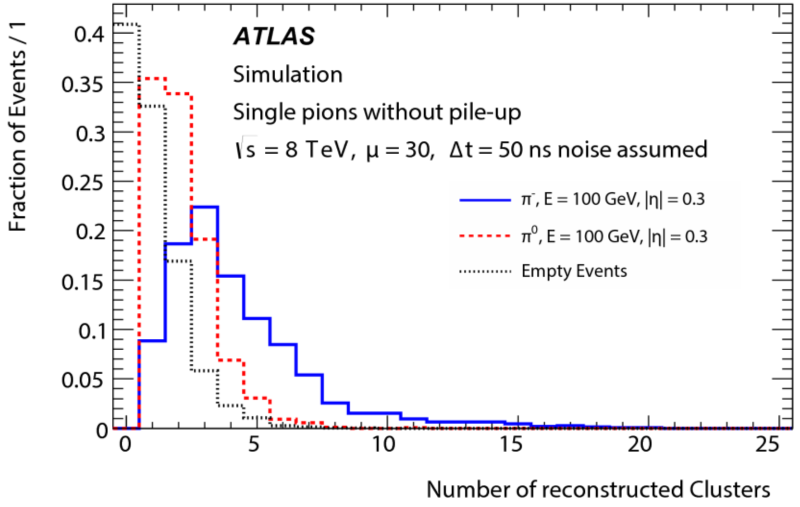

Single pions, no pile-up, noise thresholds set for 30 interations/bunch crossing, bunch distance 50 ns (early Run 1)

- Shower dependent topo-cluster yield
  - Compact EM showers split into fewer clusters than hadronic showers

Collision environment: topo-clusters do not represent individual particles, they are a proxy for energy flow generated by particles!

Topo-cluster Formation in the FCal1 Module

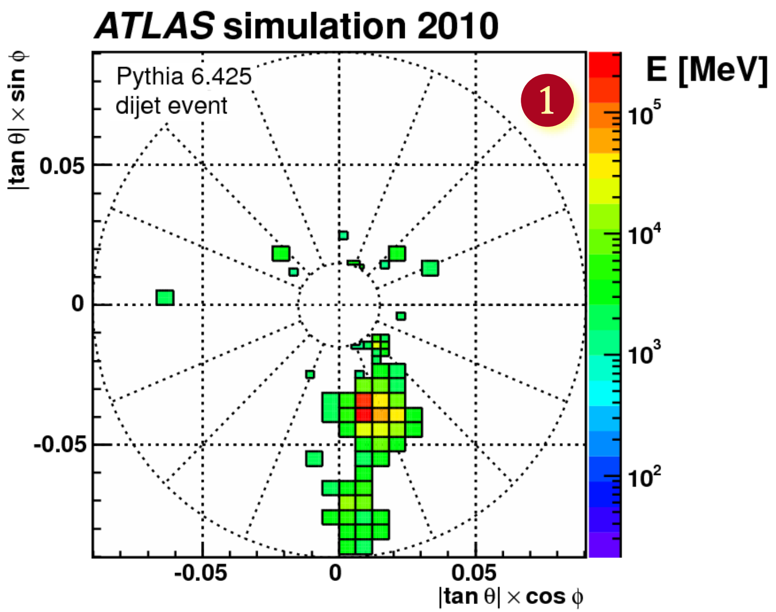

No pile-up!

Seed cells

$$\left|E^{\mathrm{EM}}_{\mathrm{cell}}\right| / \sigma^{\mathrm{EM}}_{\mathrm{noise,cell}} > 4$$

1 Initial seed collection

All cells above seed threshold

- All these cells will be clustered
- No need for neighbors with large signal significance

Topo-cluster Formation in the FCal1 Module

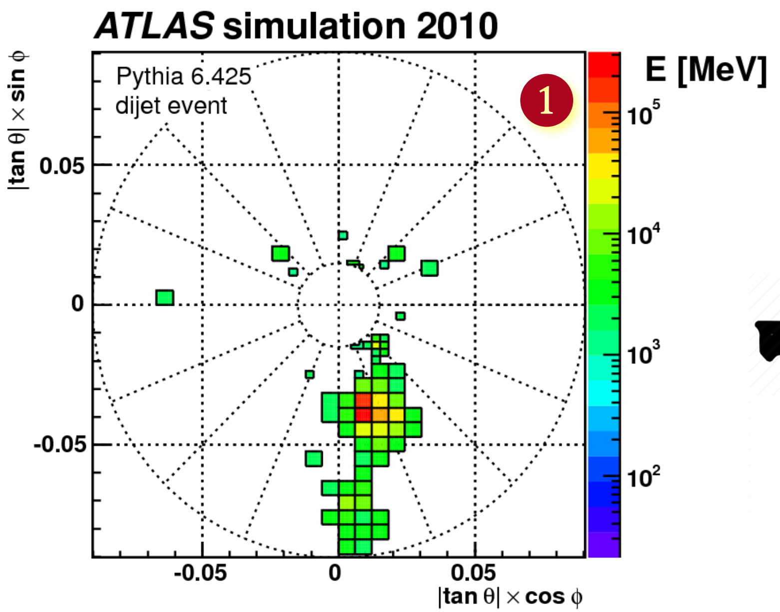

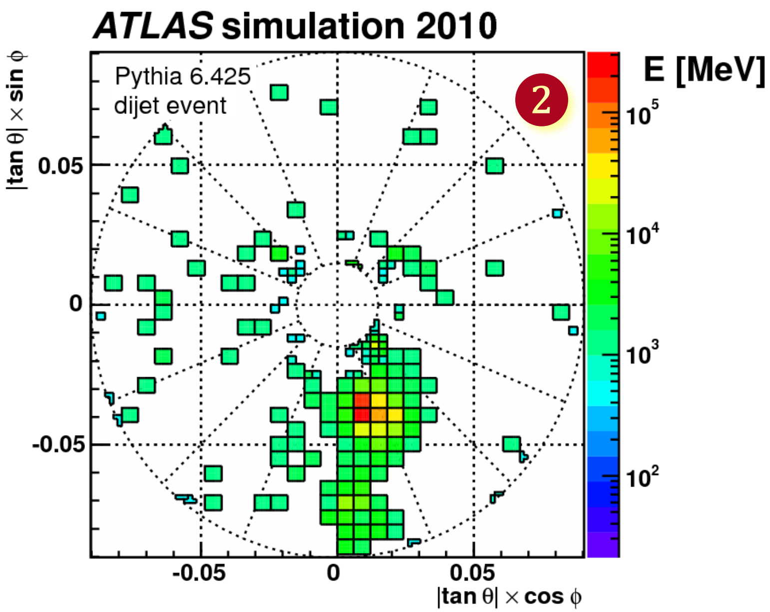

No pile-up!

Seeding

$$\left|E_{\text{cell}}^{\text{EM}}\right| / \sigma_{\text{noise,cell}}^{\text{EM}} > 4$$

Growth control cells

$$\left|E_{\text{cell}}^{\text{EM}}\right| / \sigma_{\text{noise,cell}}^{\text{EM}} > 2$$

1 Initial seed collection

- All cells above seed threshold
  - All these cells will be clustered
  - No need for neighbors with large signal significance

2 Cells above growth control threshold

- Cells potentially contributing to cluster growth
  - Not all of them end up in one!
  - No requirement of proximity to other significant signal here

Topo-cluster Formation in the FCal1 Module

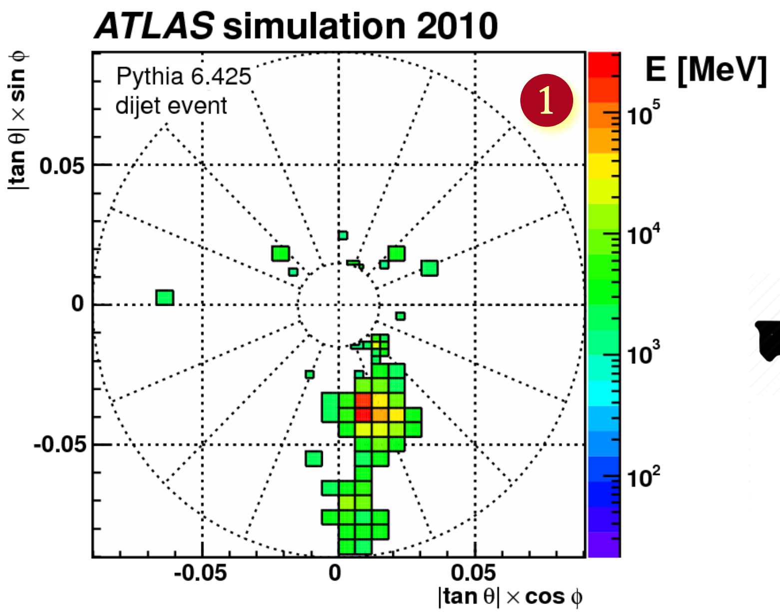

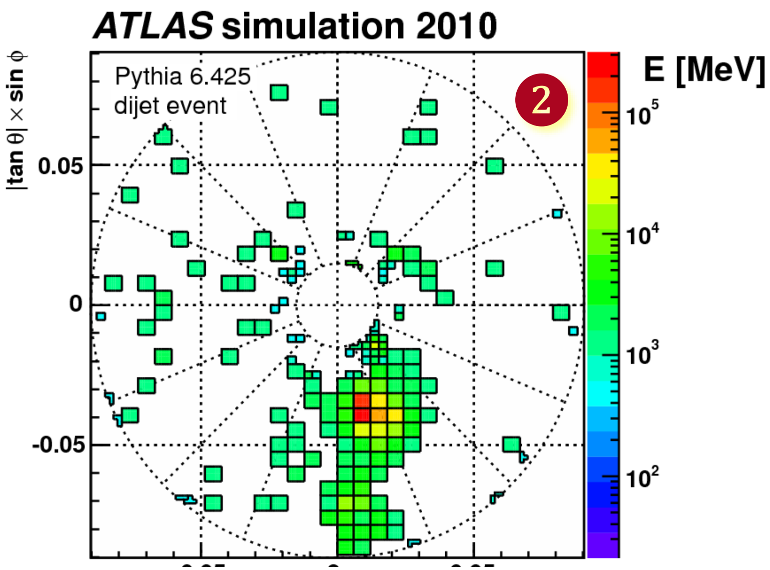

No pile-up!

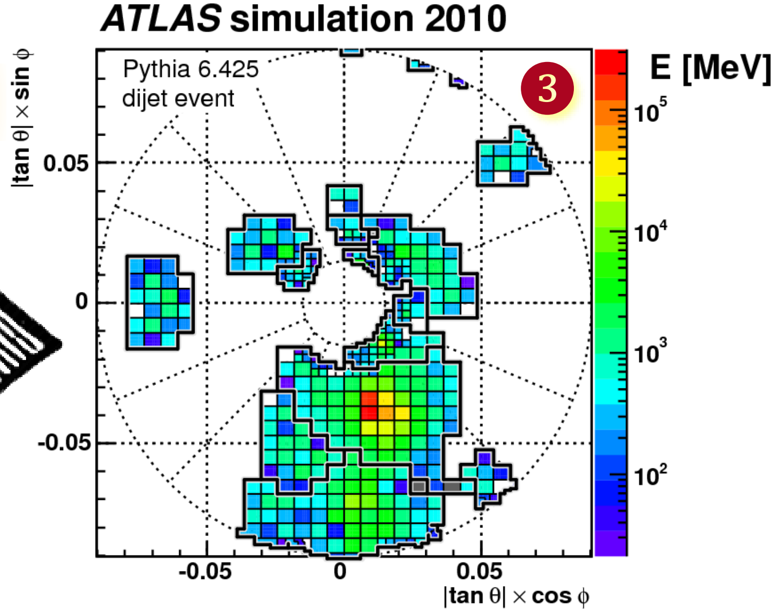

Seeding

$$|E_{\mathrm{cell}}^{\mathrm{EM}}|/\sigma_{\mathrm{noise,cell}}^{\mathrm{EM}} > 4$$

Growth control

$$|E_{\mathrm{cell}}^{\mathrm{EM}}|/\sigma_{\mathrm{noise,cell}}^{\mathrm{EM}} > 2$$

Envelope & splitting

$$|E_{\mathrm{cell}}^{\mathrm{EM}}|/\sigma_{\mathrm{noise,cell}}^{\mathrm{EM}} > 0$$

1 Initial seed collection

- All cells above seed threshold
  - All these cells will be clustered
  - No need for neighbors with large signal significance

2 Cells above growth control threshold

- Cells potentially contributing to cluster growth
  - Not all of them end up in one!
  - No requirement of proximity to other significant signal here

3 Applying neighbor requirement & splitting

- All cells collected into topo-clusters
  - According to the growth control rules
- Splitting applied
  - Distinguish energy flows induced by particles in the jet

Topo-cluster Formation in the FCal1 Module

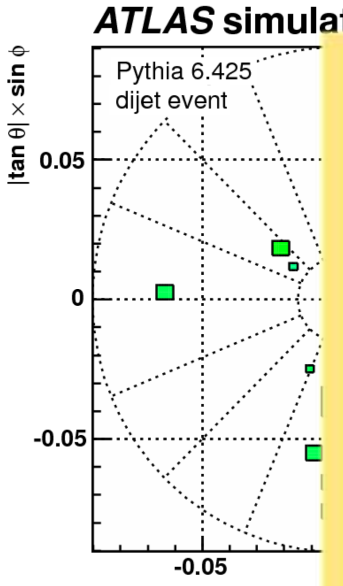

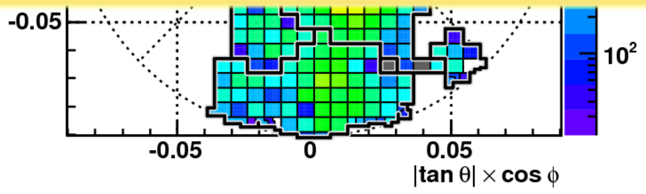

Actual implemetation in online and offline software deviates from the simplified sequence shown here! It is highly efficient, without sequential cell collections (repeated loops over cells), with only one iteration on all ~188,000 cells needed for formation, followed by one iteration on initial list of (proto-) clusters for splitting!

Seeding

$|E_{\rm cell}^{\rm EM}|/\sigma_{\rm n}^{\rm E}$ …

Growth co…

$|E_{\rm cell}^{\rm EM}|/\sigma_{\rm n}^{\rm E}$ …

Envelope & splitting

$|E_{\rm cell}^{\rm EM}|/\sigma_{\rm noise,cell}^{\rm EM} > 0$

…collection

…seed threshold

…lls will be

… neighbors with

… significance

…growth

…ld

…y contributing

…th

…em end up in one!

…nent of proximity

…nificant signal here

…ghbor

…splitting

…ed into topo-

…o the growth control rules

Splitting applied

Distinguish energy flows induced by particles in the jet

Signal Significance for Clustered Cells in ZeroBias Data

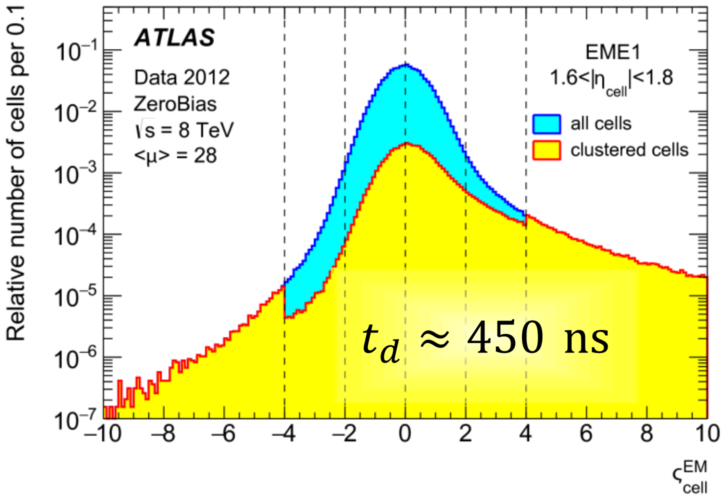

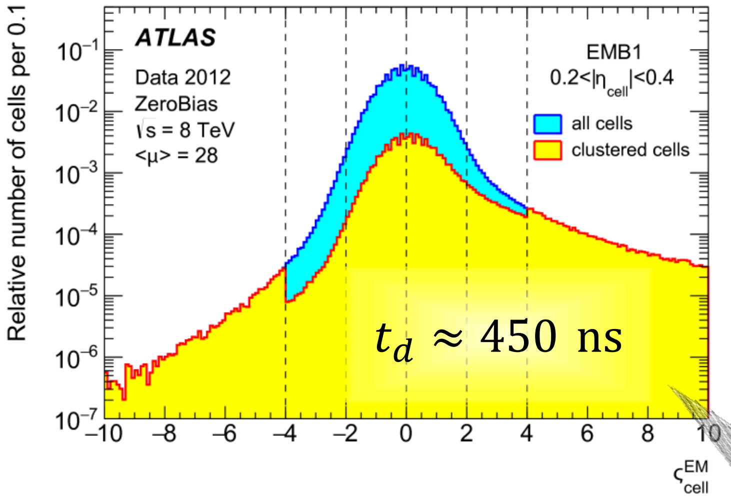

Tails in cell significance introduced by physics – with contributions from in-time minimum bias collisions and correlations in out-of-time pile-up signal remnants

2012 data with pile-up!

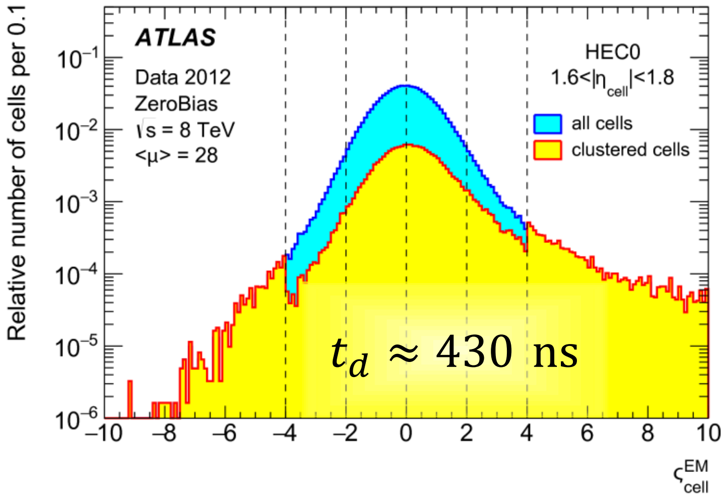

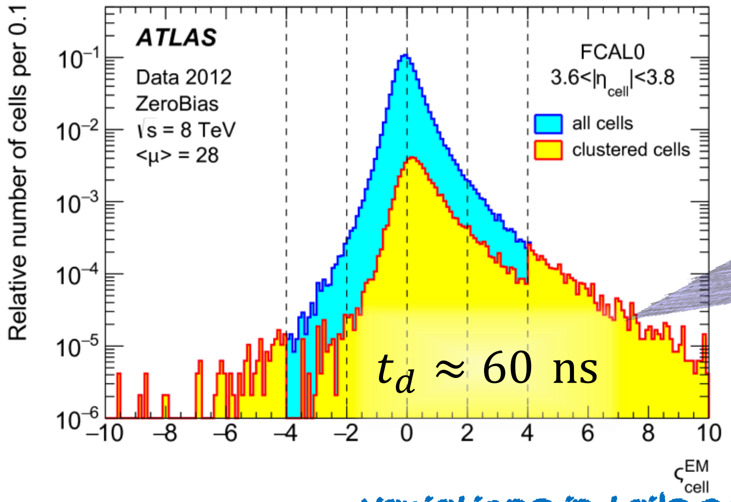

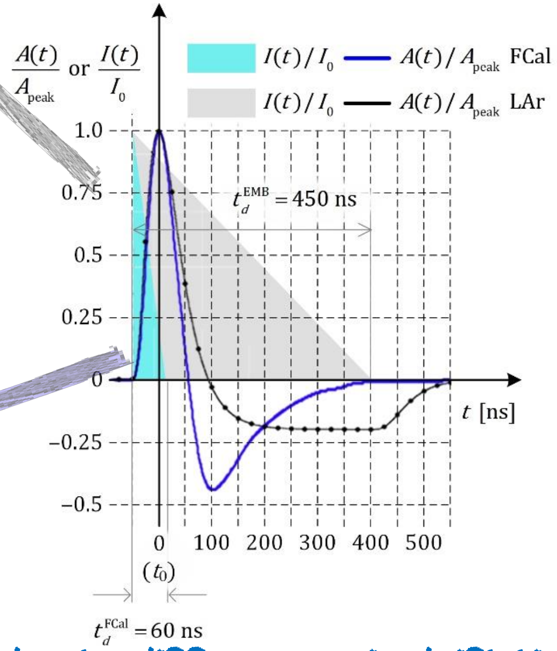

Variations in tails partly due to differences in drift time (LAr gap sizes) leading to different pulse shapes

Topo-cluster Moments/Features

Principal geometry

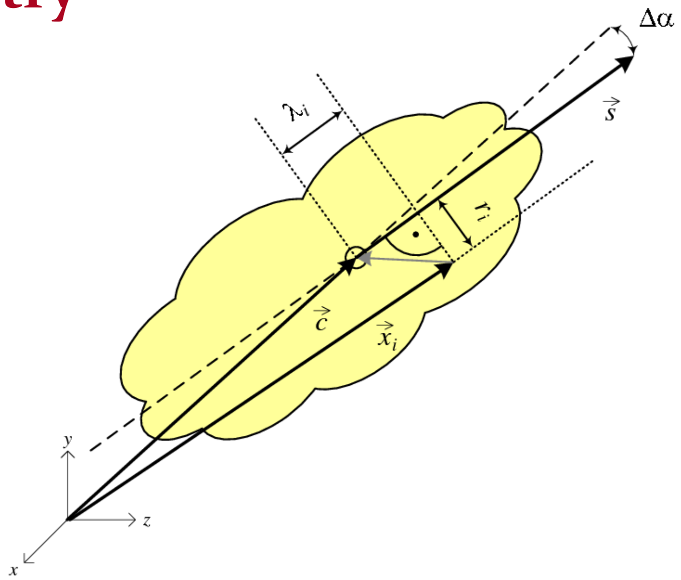

- $\vec{c}$ *centre of gravity of cluster, measured from the nominal vertex* ($x = 0, y = 0, z = 0$) *in ATLAS*
- $\vec{x}_i$ *geometrical centre of a calorimeter cell in the cluster, measured from the nominal detector centre of ATLAS*
- $\vec{s}$ *particle direction of flight (shower axis)*
- $\Delta\alpha$ *angular distance* $\Delta\alpha = \angle(\vec{c}, \vec{s})$ *between cluster centre of gravity and shower axis* $\vec{s}$
- λ_i *distance of cell at* $\vec{x}_i$ *from the cluster centre of gravity measured along shower axis* $\vec{s}$ ($\lambda_i < 0$ *is possible*)
- r_i *radial (shortest) distance of cell at* $\vec{x}_i$ *from shower axis* $\vec{s}$ ($r_i \geq 0$)

Cluster moments (features)

- Energy-weighted first and second moments
  - Lateral and longitudinal extensions (normalized and absolute)
  - Signal density measure
- Signal relevance and compactness measures
  - Signal significance
  - EM/HAD energy sharing

Location & environment

- Position and direction
  - Depth of topo-cluster in calorimeter
  - Distance from vertex
  - Angular deflection from vertex direction
- Environment
  - Isolation

Local Hadronic Calibration (LCW)

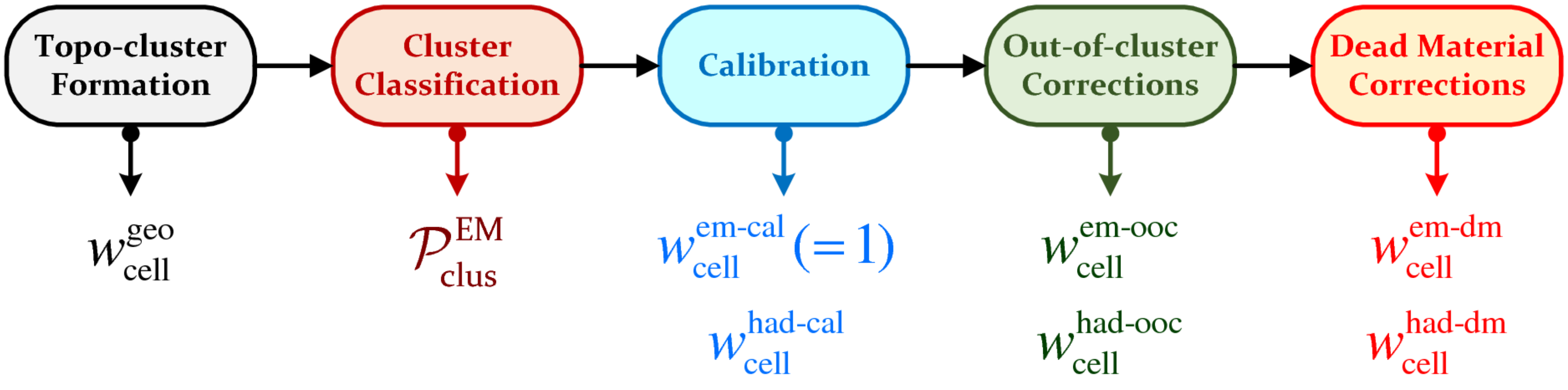

Local cluster calibration

- Uses cluster shape and location to apply appropriate calibrations
  - Observables are proxies for shower shapes – sensitive to electromagnetic or hadronic shower development
- Calibration reference is deposited energy at cluster location
  - Additional corrections for nearby dead material losses and out-of-cluster losses (includes isolation measure)
- All calibration functions are derived from full single particle simulations
  - Direction and energy scans with π^0, $\pi^\pm$ – **no pile-up included**
  - Deposited energies collected in clusters formed with $\langle\mu\rangle$ dependent $\sigma_{\text{noise,cell}}^{\text{EM}}$
  - Calibration factors stored in multi-dimensional lookup tables
- Final cluster representation
  - Massless four-momentum $(E, \eta, \varphi, m = 0)$ on EM and LCW scale

LCW: Classification

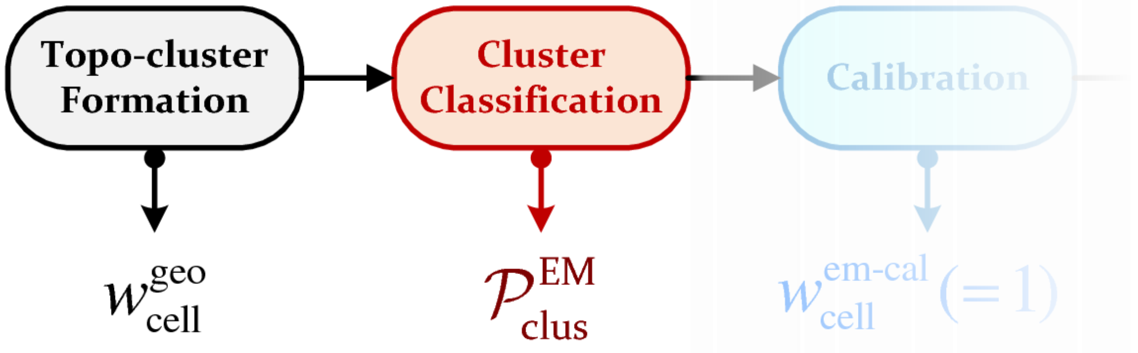

Jet fragmentation modeling

⊗ shower starting point & longitudinal profile

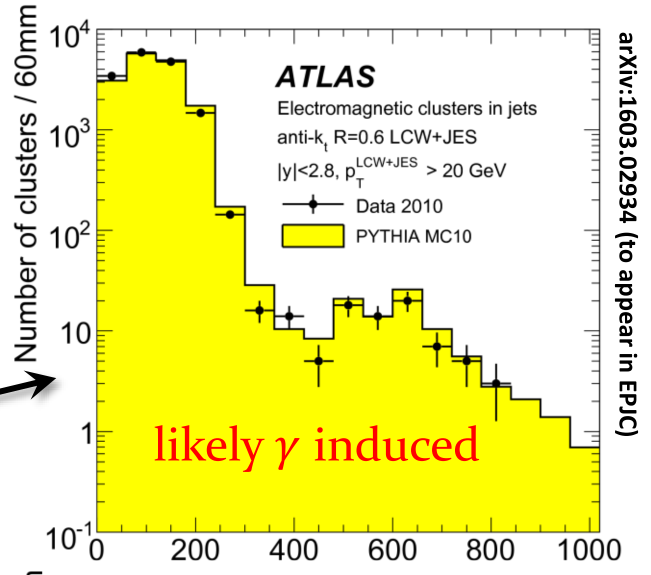

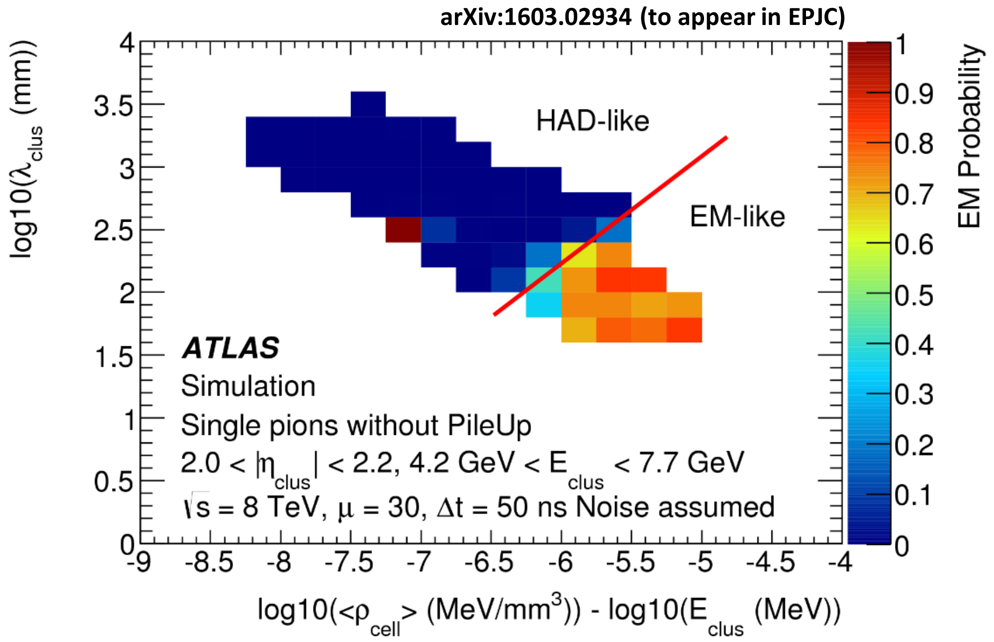

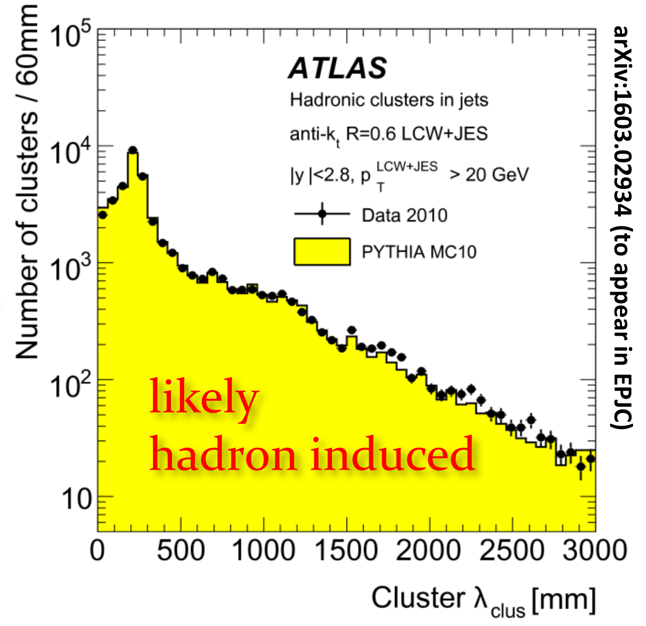

Peter Loch

LCW: Hadronic Calibration

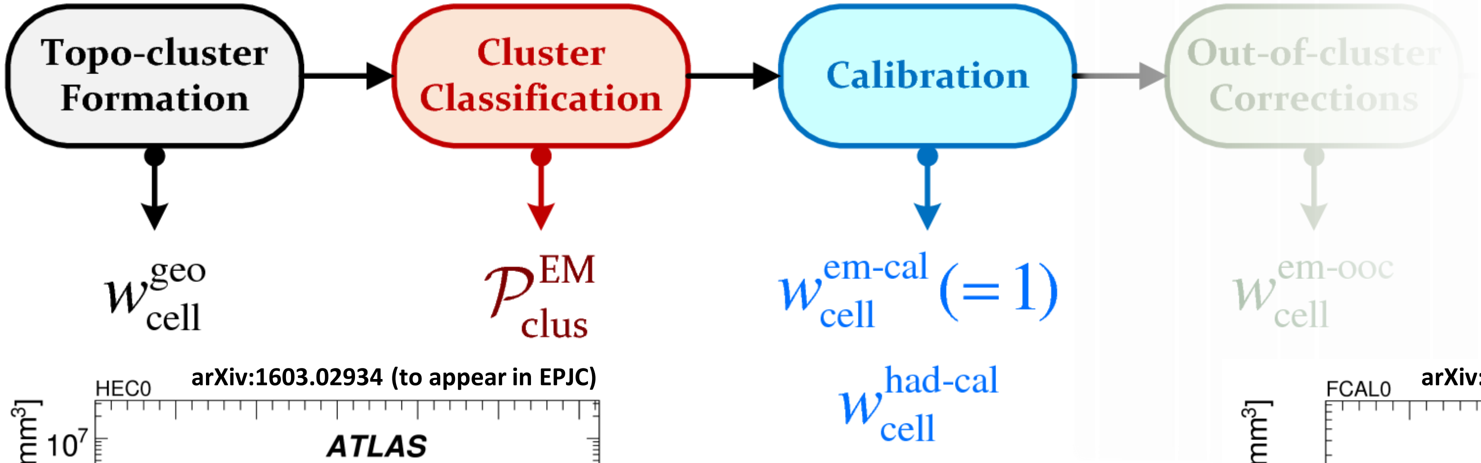

arXiv:1603.02934 (to appear in EPJC)

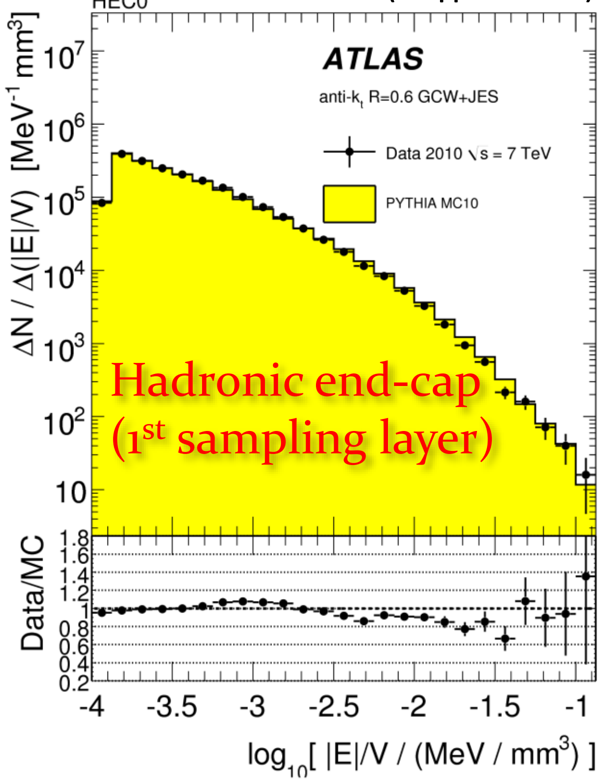

Jet fragmentation modeling
⊗ shower development

arXiv:1603.02934 (to appear in EPJC)

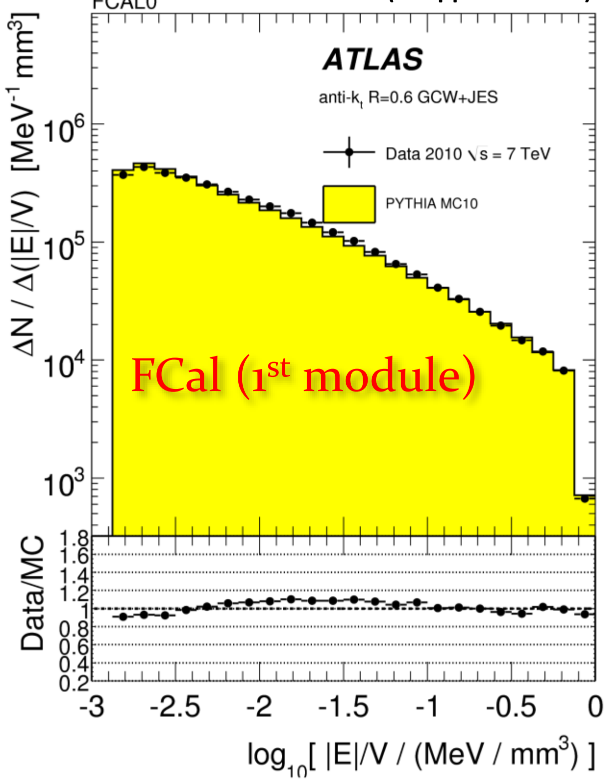

LCW: Out-of-cluster Correction

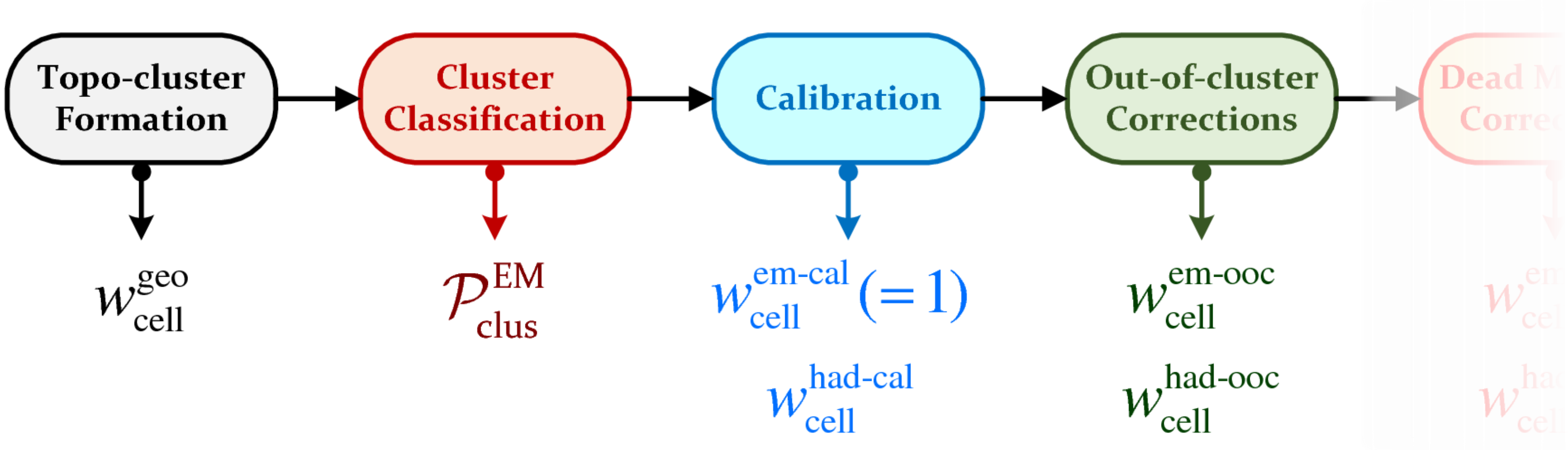

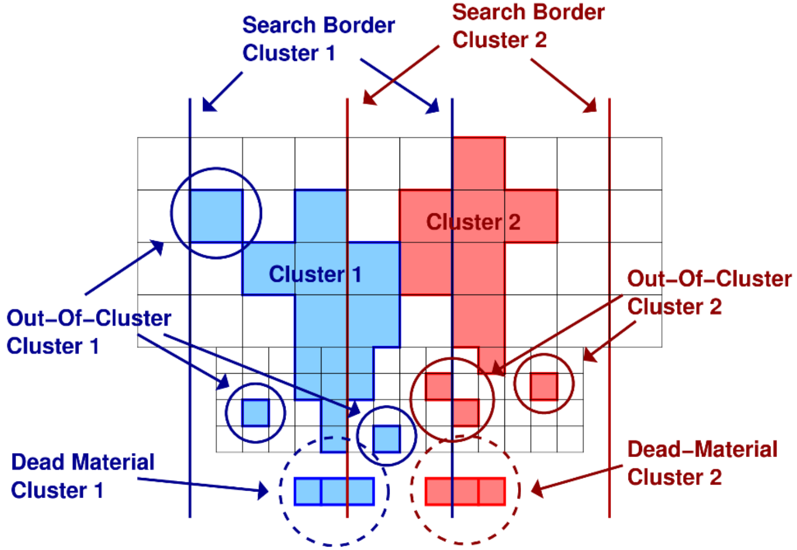

arXiv:1603.02934 (to appear in EPJC)

arXiv:1603.02934 (to appear in EPJC)

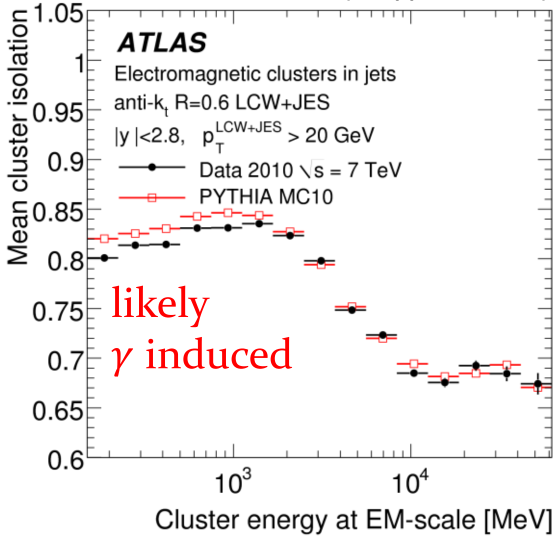

arXiv:1603.02934 (to appear in EPJC)

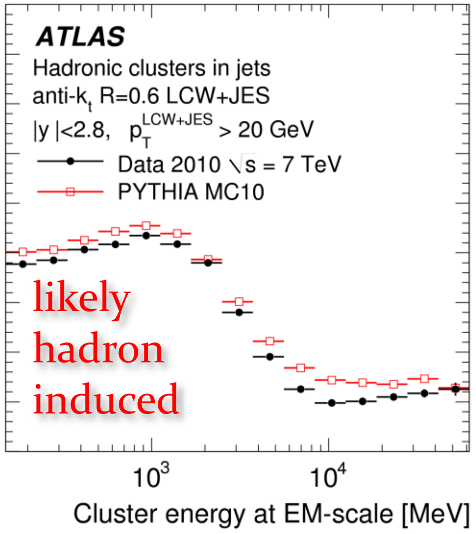

LCW: Dead Material Correction

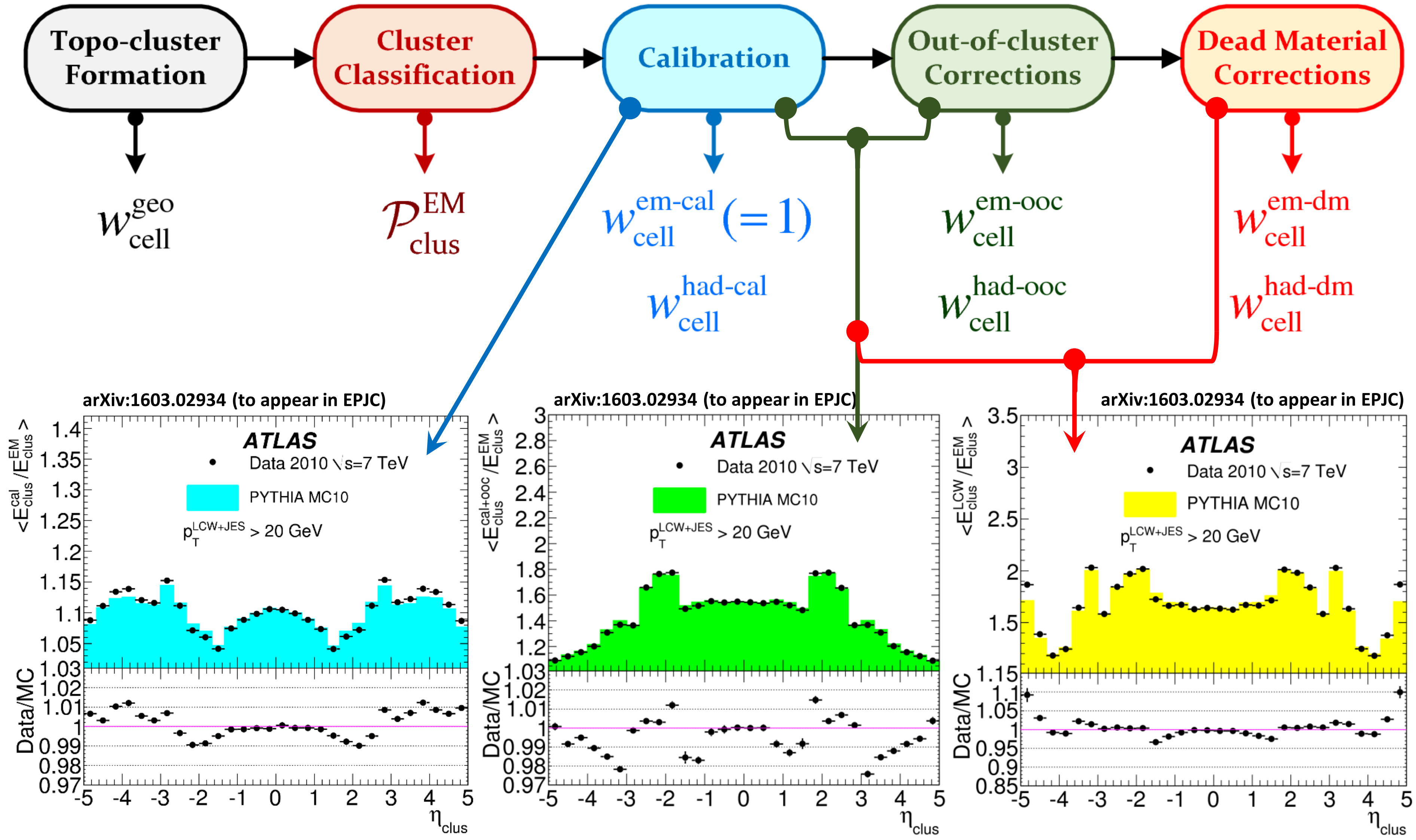

Peter Loch

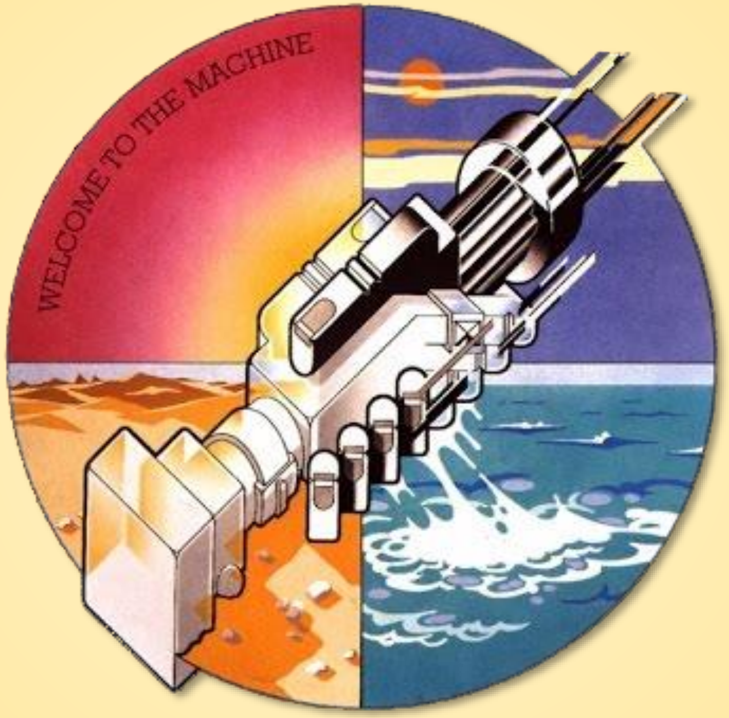

WELCOME TO THE MACHINE !

Conclusions & Outlook

ATLAS Calorimeters

- Successfully operating since 2010
  - Highly efficient and stable system
- Highly optimized for total absorption
  - Precise energy flow reconstructions for jets, event shapes, hadronic recoil etc. in both *pp* (with increasing levels of pile-up) and heavy ion collision environments
- Effective signal definition – topo-clusters and topo-towers
  - Drop a large amount of “noise only” cells at early stage of reconstruction
  - Pile-up suppression due to detector readout and adaptive signal significance thresholds
  - Present day local hadronic calibration needs improvements – machine-learning-based approaches under study (see recent JetEtMiss PubNote)

Future challenges

- Hi-lumi LHC pile-up
  - Cluster formation/splitting sufficient to maintain precision in energy flow reconstruction?
  - More use of/combination with topo-towers?
- Machine learning for cluster formation and calibration
  - Several approaches under study
  - Biases and gains not yet obvious for formation,

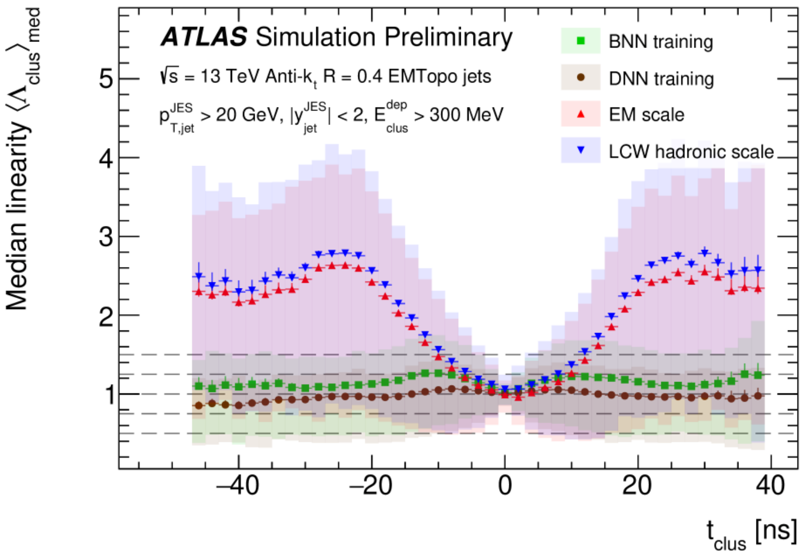

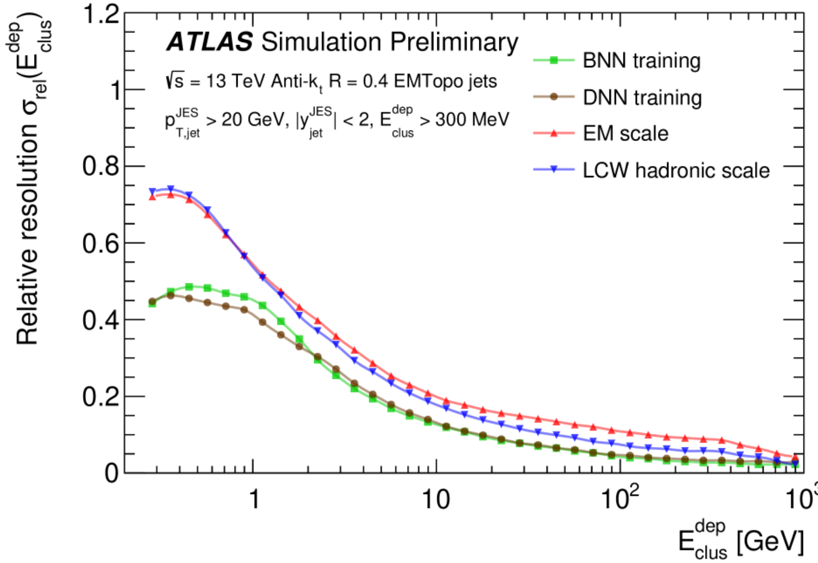

Next for me…. Looking for new experiment!

- Expected final state components:

Next for me…. Looking for new experiment!

- ❖ Expected final state components:

  - ⁜ Not observed yet – needs clean up and calibration

Next for me…. Looking for new experiment!

❖ Expected final state components:

※ Not observed yet – needs clean up and calibration

※ Fine tuning and calibration (observed!)

Next for me…. Looking for new experiment!

❖ Expected final state components:

※ Not observed yet – needs clean up and calibration

※ Fine tuning and calibration (observed!)

❖ Leadership & location

※ Research & Spokesperson (elected for life, already in place)

※ Location

Next for me…. Looking for new experiment!

- Expected final state components:

  - Not observed yet – needs clean up and calibration

  - Fine tuning and calibration (observed!)

- Leadership & location

  - Research & Spokesperson (elected for life, already in place)

  - Location

Additional Material

Click here!

https://indico.cern.ch/event/1366444/attachments/2781618/4879898/Atlas.02.06.2024%20-%20Additional%20material.pdf

LCW Cell Weights

- Full topo-cluster calibration is projected back on cell weights
  - EM likelihood $\mathcal{P}_{\text{clus}}^{\text{EM}}$ defines EM/HAD mixture of factors
    - $\mathcal{P}_{\text{clus}}^{\text{EM}} = 1$ for pure EM clusters, $\mathcal{P}_{\text{clus}}^{\text{EM}} = 0$ for pure HAD
  - Hadronic calibration & dead material correction produce individual cell weights

Procedure	Parameters	Effective cell signal weight after each step
(1) Cluster formation	$w_{\text{cell}}^{\text{geo}}$	$w_{\text{cell}}^{\text{geo}}$
(2) Classification	$\mathcal{P}_{\text{clus}}^{\text{EM}}$	$w_{\text{cell}}^{\text{geo}}$
(3) Calibration	$w_{\text{cell}}^{\text{em-cal}} (= 1)$ $w_{\text{cell}}^{\text{had-cal}}$	$w_{\text{cell}}^{\text{geo}} \left[\mathcal{P}_{\text{clus}}^{\text{EM}} \, w_{\text{cell}}^{\text{em-cal}} + (1 - \mathcal{P}_{\text{clus}}^{\text{EM}}) \, w_{\text{cell}}^{\text{had-cal}} \right]$
(4) Out-of-cluster	$w_{\text{cell}}^{\text{em-ooc}}$ $w_{\text{cell}}^{\text{had-ooc}}$	$w_{\text{cell}}^{\text{geo}} \prod_{\kappa \in \{\text{cal,ooc}\}} \left[\mathcal{P}_{\text{clus}}^{\text{EM}} \cdot w_{\text{cell}}^{\text{em}-\kappa} + (1 - \mathcal{P}_{\text{clus}}^{\text{EM}}) \cdot w_{\text{cell}}^{\text{had-}\kappa} \right]$
(5) Dead material	$w_{\text{cell}}^{\text{em-dm}}$ $w_{\text{cell}}^{\text{had-dm}}$	$w_{\text{cell}}^{\text{LCW}} = w_{\text{cell}}^{\text{geo}} \prod_{\kappa \in \{\text{cal,ooc,dm}\}} \left[\mathcal{P}_{\text{clus}}^{\text{EM}} \, w_{\text{cell}}^{\text{em}-\kappa} + (1 - \mathcal{P}_{\text{clus}}^{\text{EM}}) \, w_{\text{cell}}^{\text{had-}\kappa} \right]$

Calorimeter Topo-tower Revival

- Provide different view on energy flow

(from P.A. Delsart)

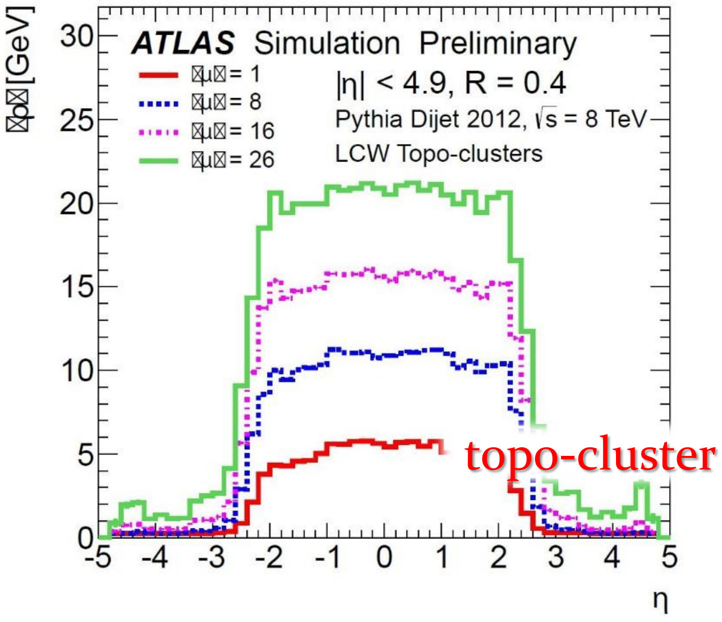

topo-cluster

$\mapsto N^{\mathrm{jet}}_{\mathrm{constituent}} = 1$
(low noise signal)

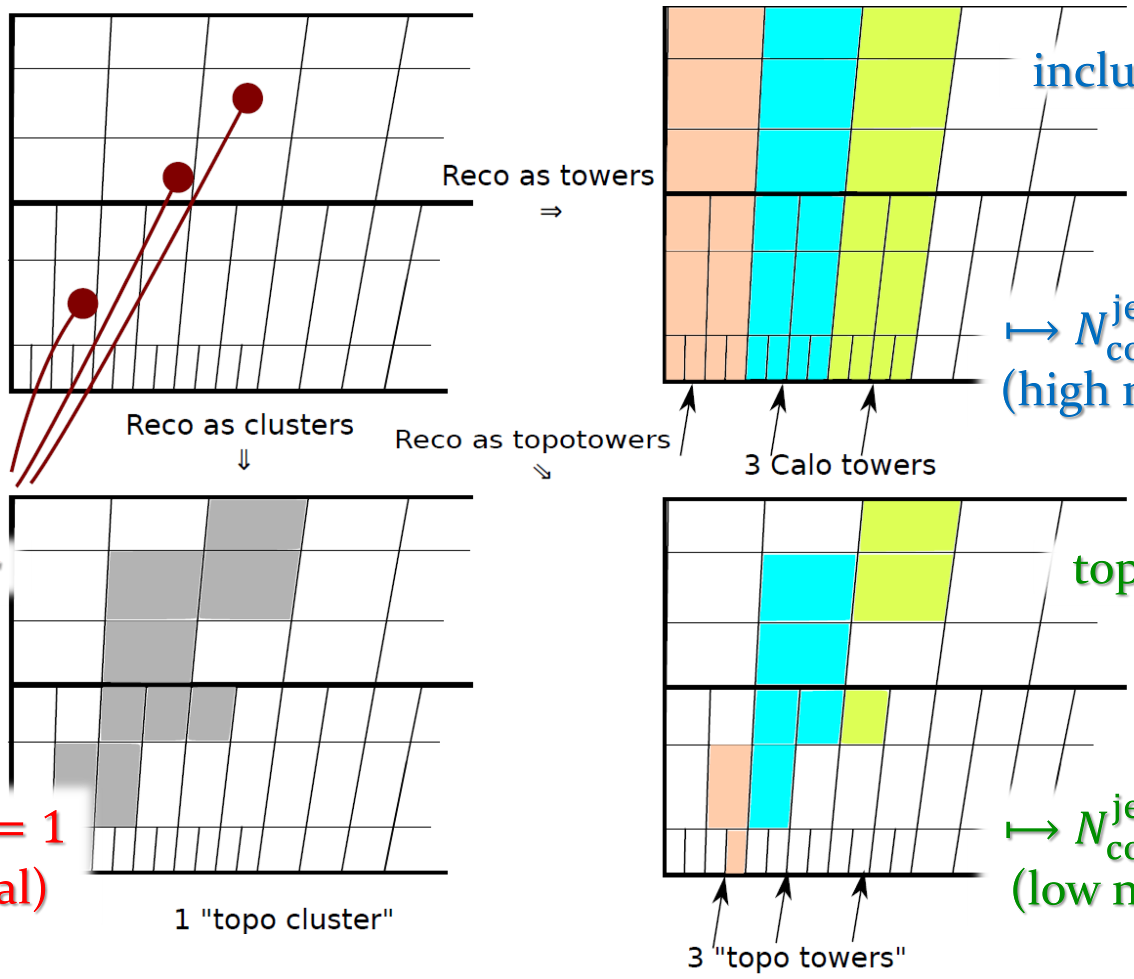

inclusive towers

$\mapsto N^{\mathrm{jet}}_{\mathrm{constituent}} = 3$
(high noise signal)

topo-towers

$\mapsto N^{\mathrm{jet}}_{\mathrm{constituent}} = 3$
(low noise signal)

Calorimeter Topo-tower Revival

- New for Run3
  - Drop of calorimeter granularity at $|\eta| > 2.5$
    - Few topo-clusters formed from large cells
    - Energy flow highly discrete – large voids in (y, φ) plane, sparse four-momentum occupancy
    - Median transverse momentum density measurement deteriorates
  - Re-introduce calorimeter towers
    - Imposes different view on non-projective FCal readout
    - Well-defined catchment area for area-based pile-up suppression algorithms $\Delta y \times \Delta\varphi = 0.1 \times 0.1$
    - Uses only cells from topo-clusters (noise suppression identical)

Misses 16 cells in FCal3 with > 19 towers (not included in graph but mapped in database)

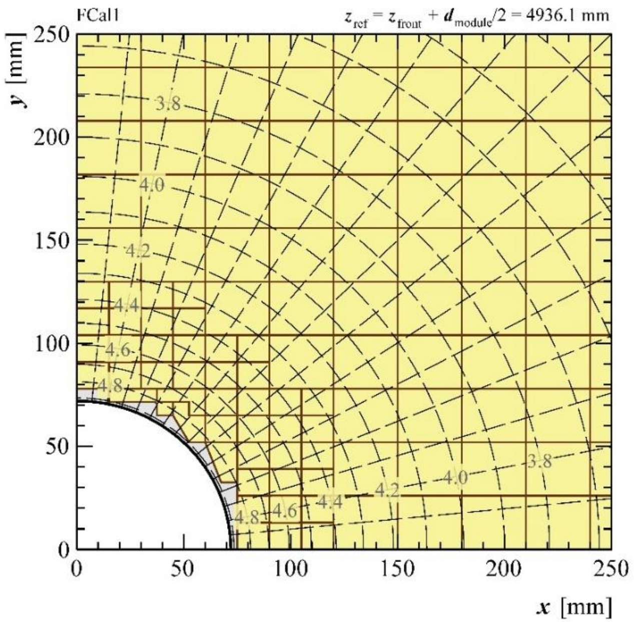

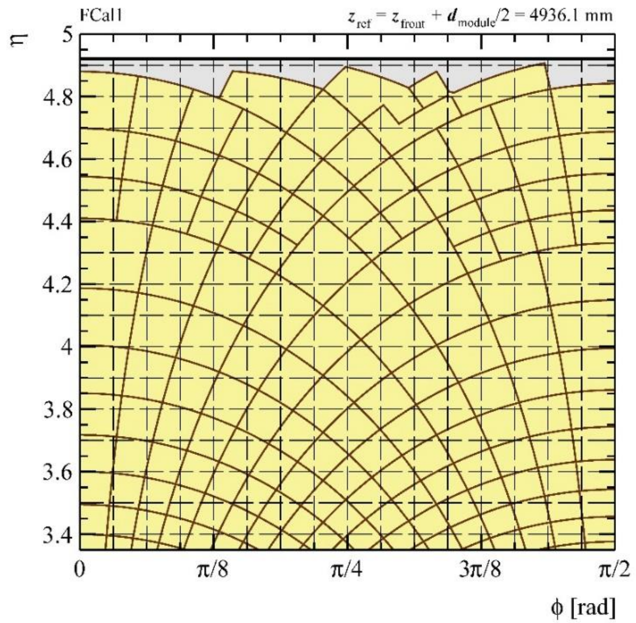

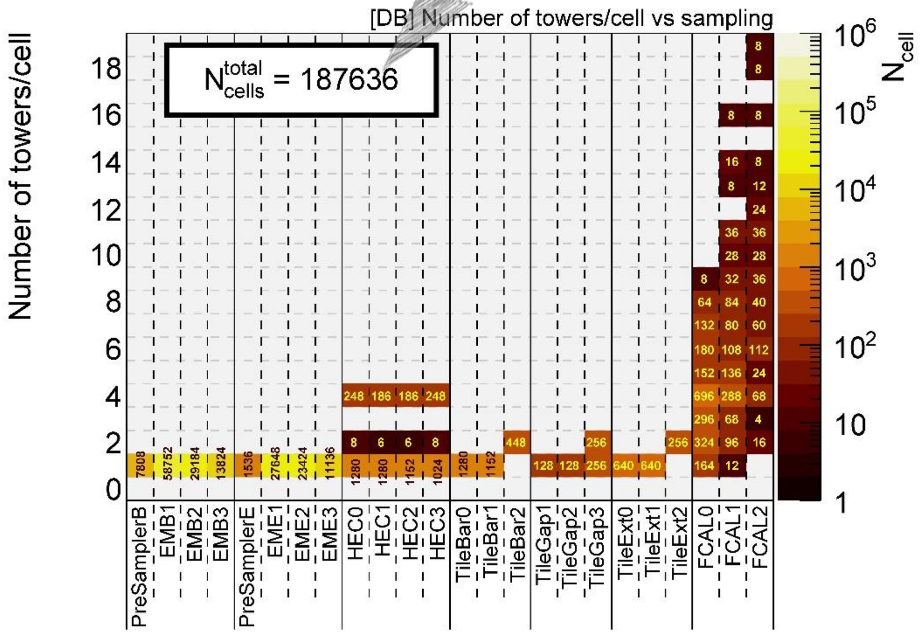

Calorimeter Topo-towers

- Considerations
  - Topo-towers are represented by the same data object as topo-clusters
    - Possible to add moments (not all are meaningful for towers)
  - Large amount of data to be stored
    - Inclusive towers (all cells) completely impractical
    - Too many topo-towers (from cells after noise suppression)
- Topo-towers in the AOD
  - Only for $|\eta| > 2.5$ - ForwardTopoTowers
    - No (cell) signal overlap with topo-clusters with $|\eta| < 2.5$ – can be combined for unambiguous energy flow reconstruction
  - Ghost-associated with jets
    - Support pile-up jet suppression outside of tracking aceptance

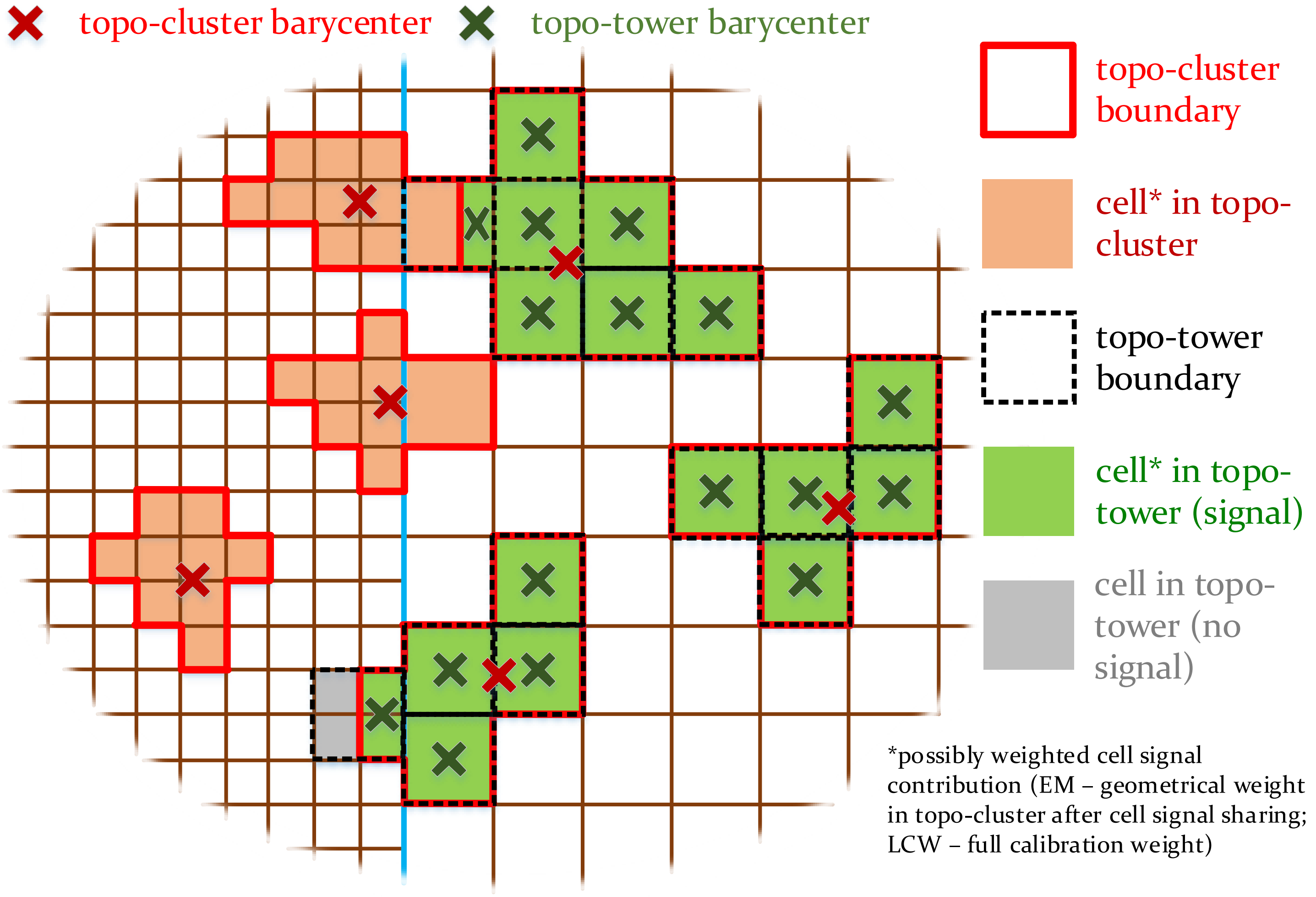

*possibly weighted cell signal contribution (EM – geometrical weight in topo-cluster after cell signal sharing; LCW – full calibration weight)

Calorimeter Topo-towers

- Calorimeter signal multiplicities

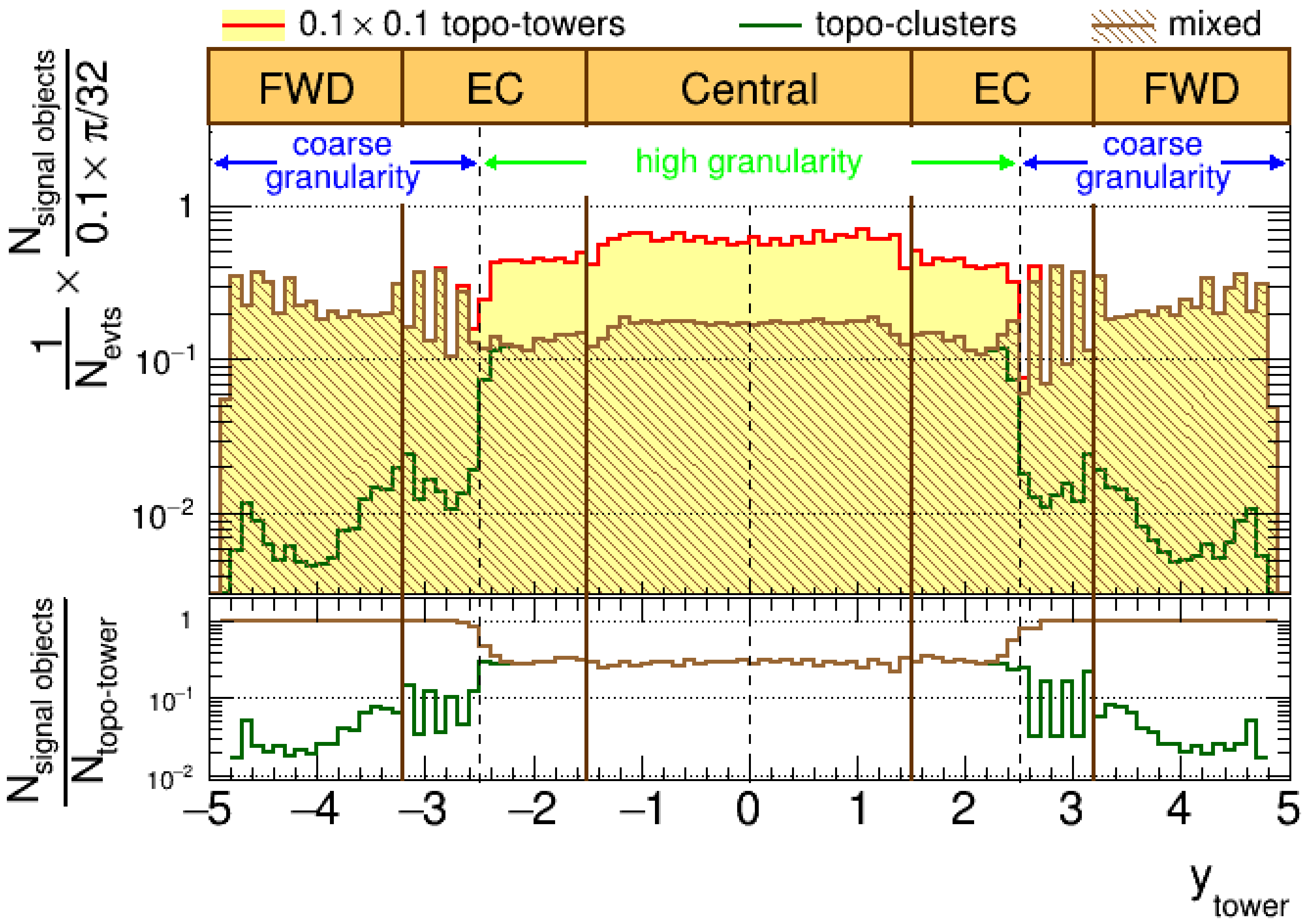

Examples of MC Modeling

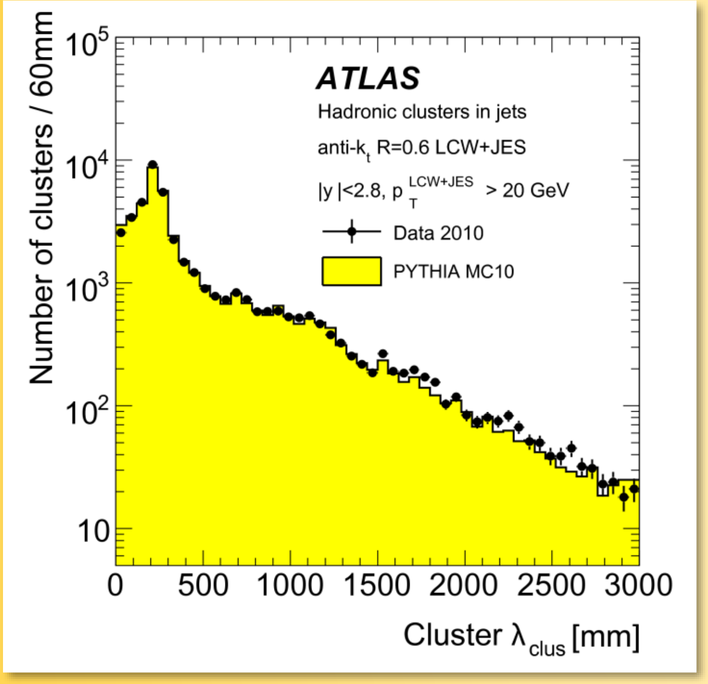

Inclusive spectrum of λ_{clus}

(topo-clusters in jets)

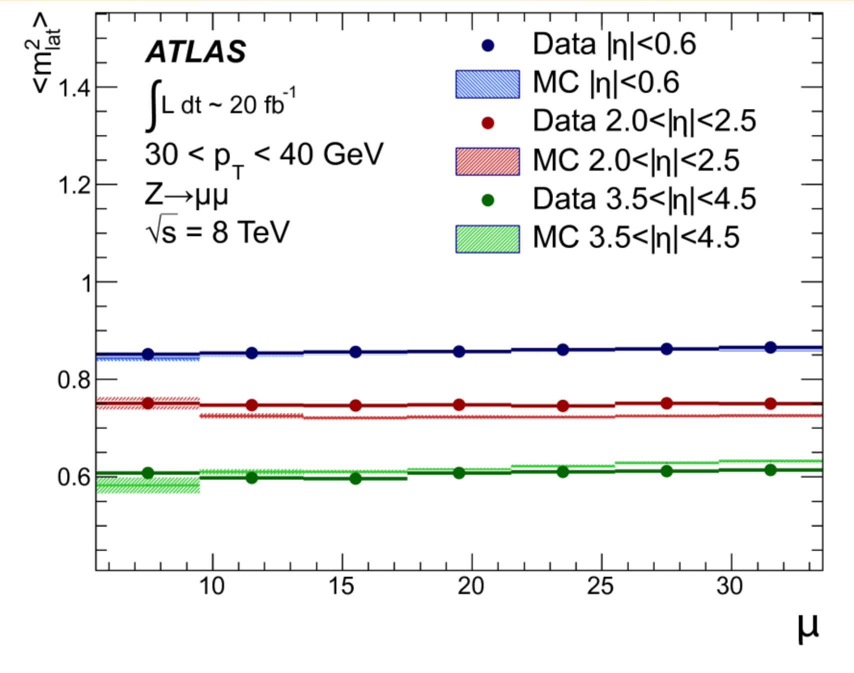

Pile-up dependence of $\langle m^2_{\mathrm{lat}} \rangle$

(topo-cluster in jets)

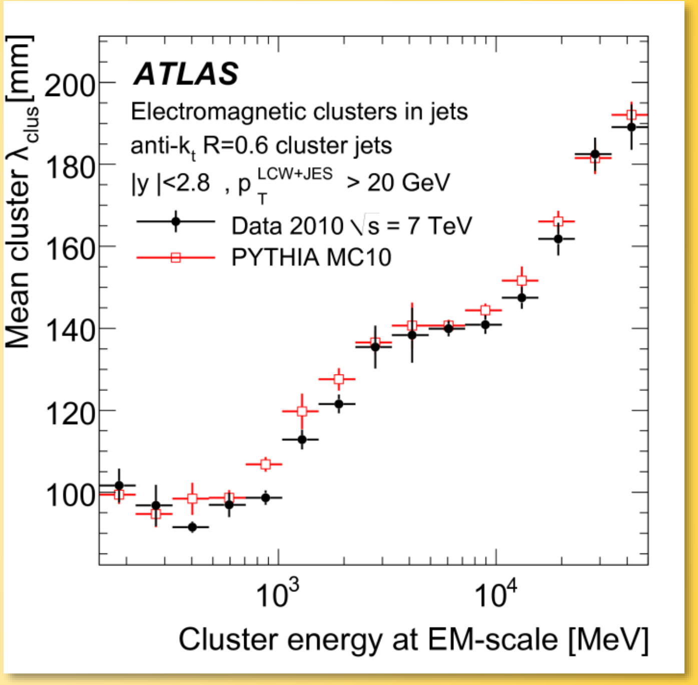

Dependence of $\langle \lambda_{\mathrm{clus}} \rangle$ on $E^{\mathrm{EM}}_{\mathrm{clus}}$

(topo-clusters in jets)

MC Modeling Problems

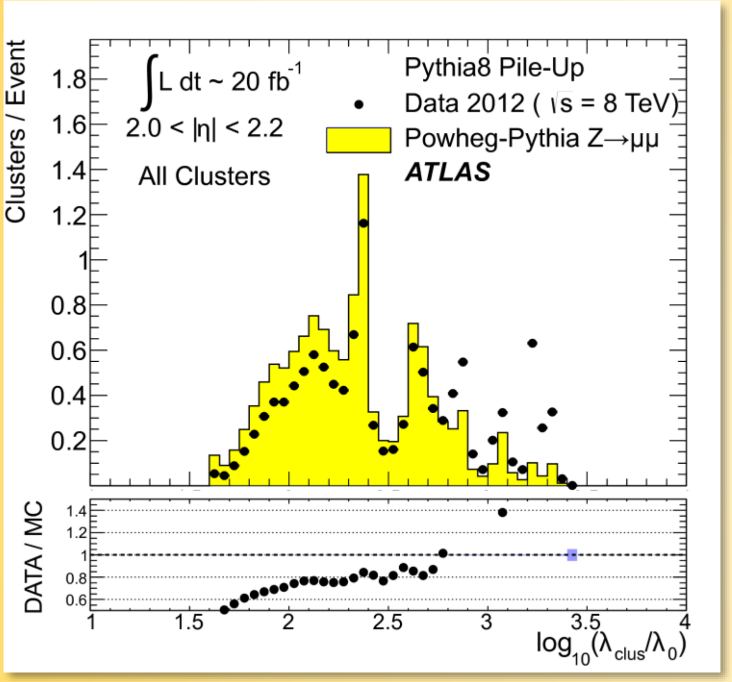

log(λ_{clus}) distribution of inclusive topo-cluster sample (no jet environment required)

(pile-up insufficiently modeled by MC generator & detector simulation)

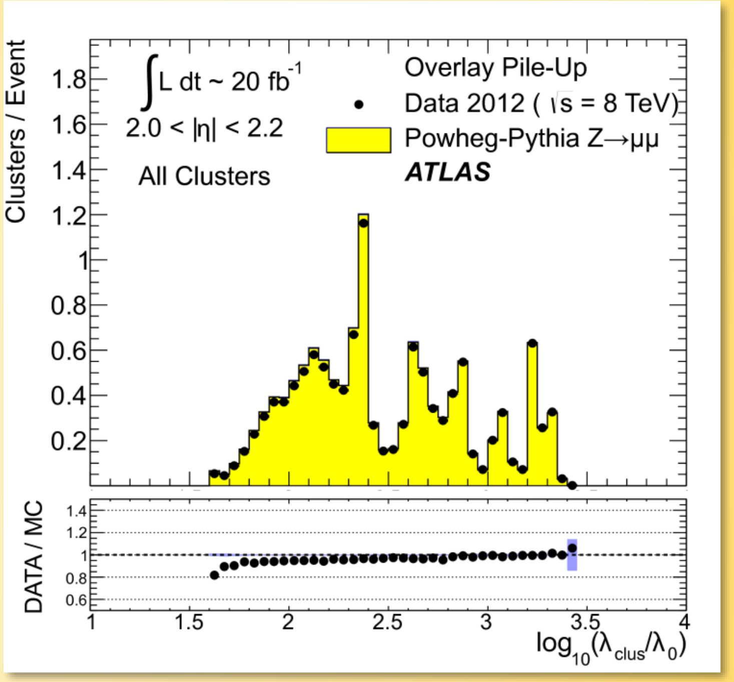

log(λ_{clus}) distribution of inclusive topo-cluster sample (no jet environment required)

(pile-up from data overlaid on hard scatter MC simulation)

Feature Choices

inclusive (all topo-clusters)

< 10% electromagnetic energy deposit

> 90% electromagnetic energy deposit

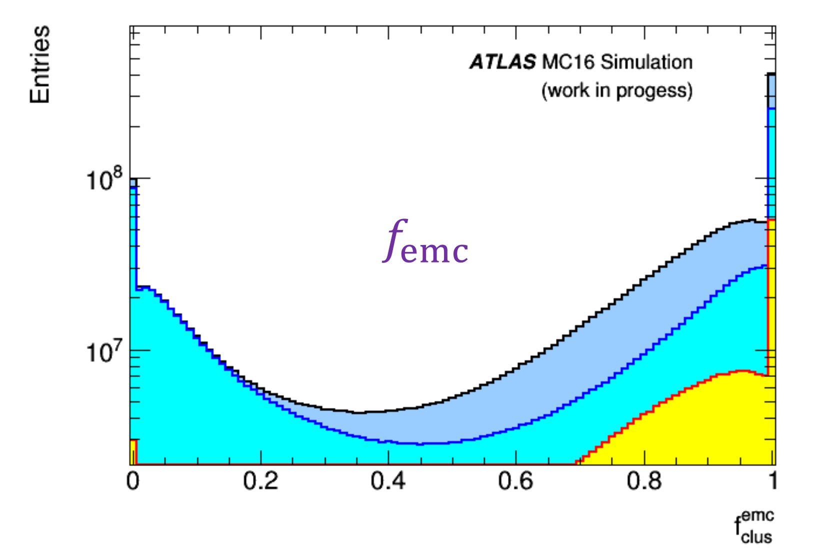

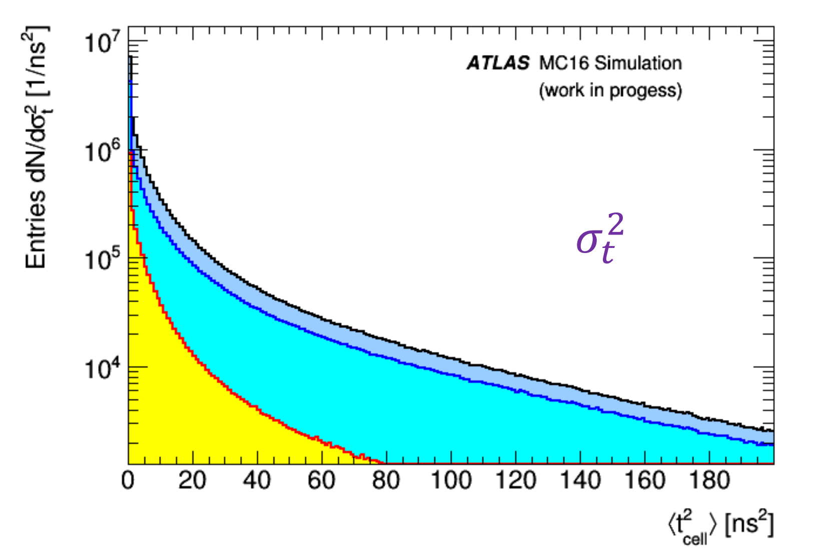

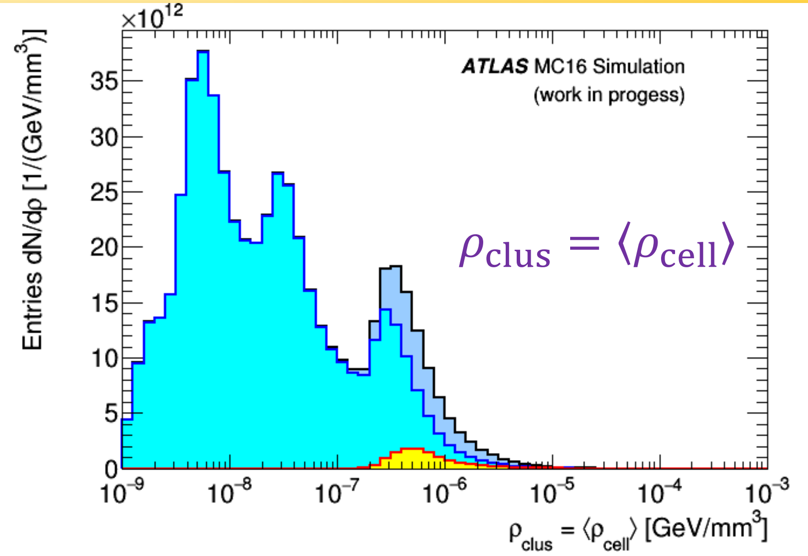

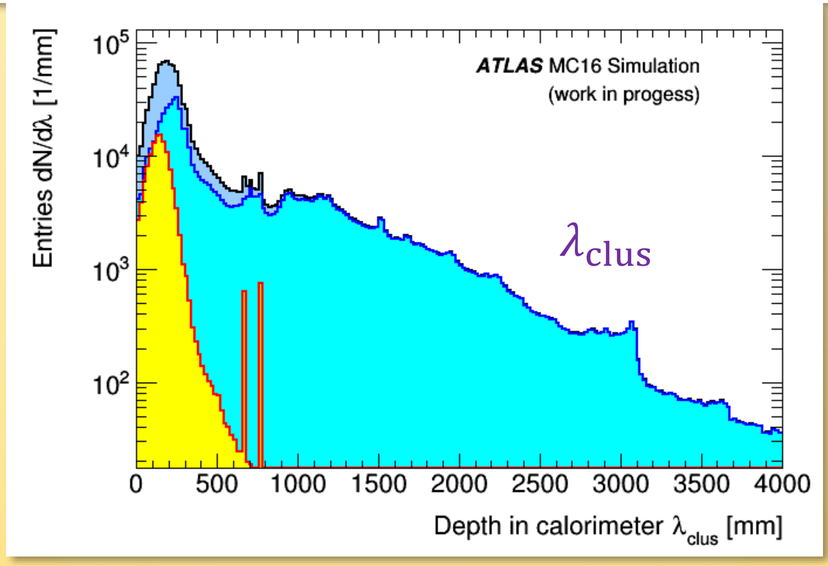

Feature Choices

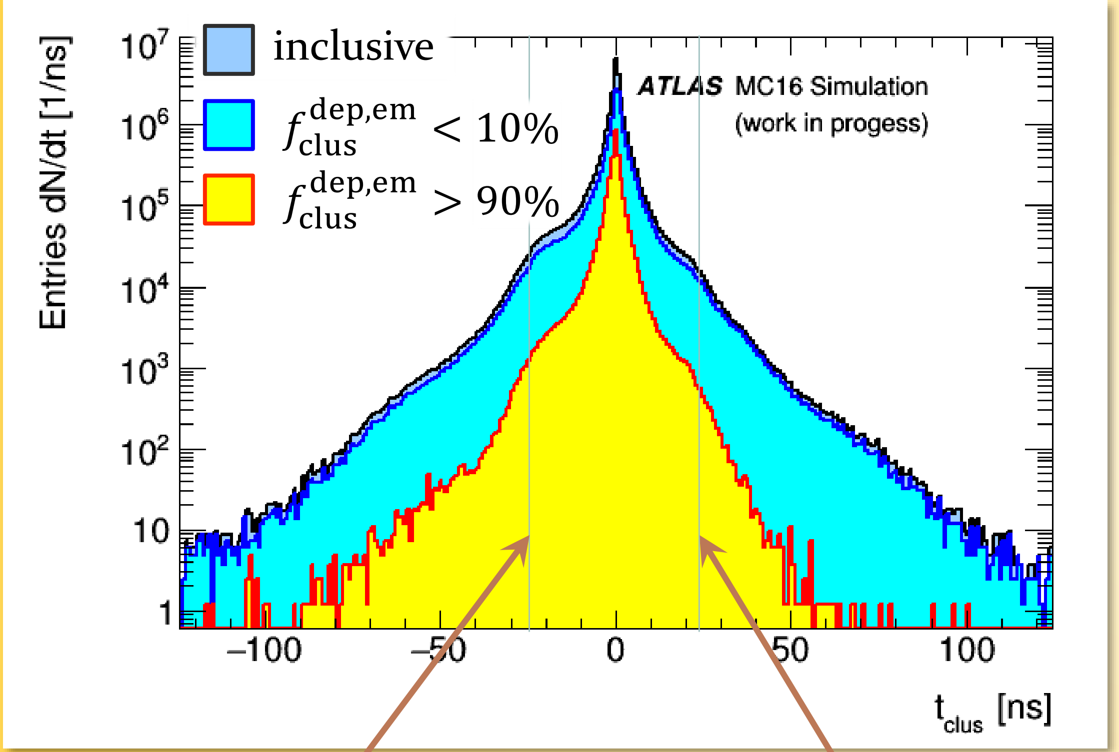

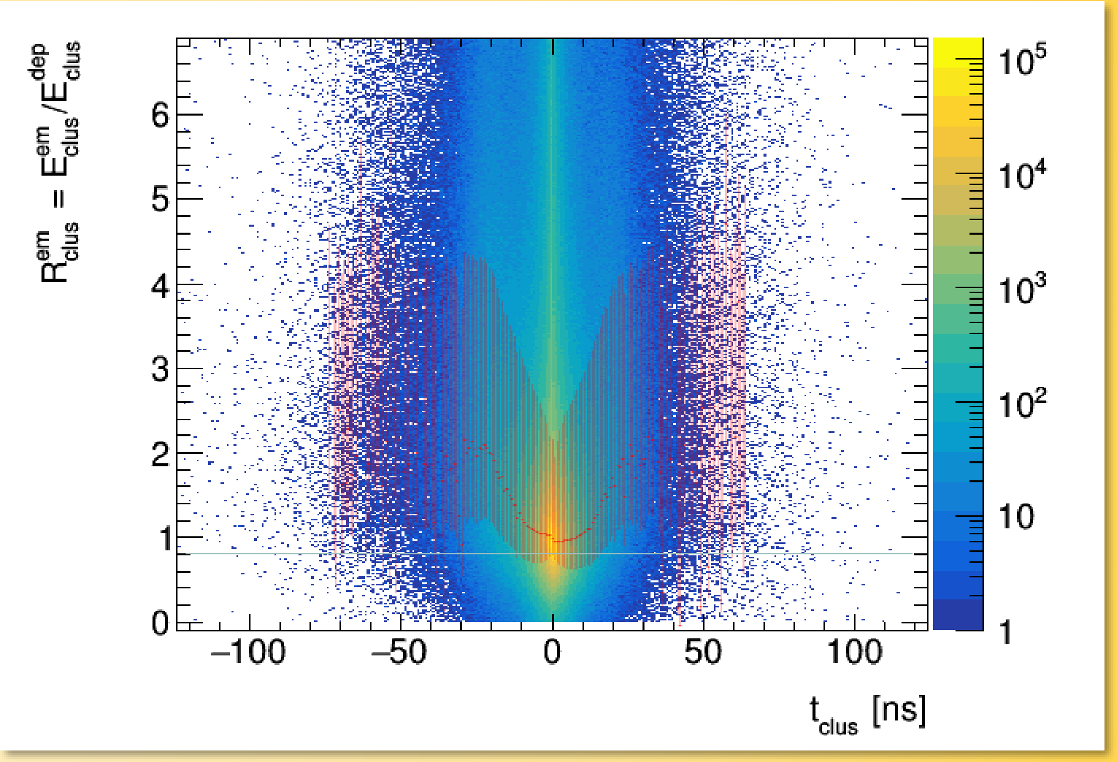

Past out-of-time pile-up signal dominance in topo-cluster at $t_{clus}(= 0) - 25$ ns

Future out-of-time pile-up signal dominance in topo-cluster at $t_{clus}(= 0) + 25$ ns

Response driven by out-of-time pile-up contributions: net additional signal gain for $t_{clus} \lesssim - 12.5$ ns and $t_{clus} \gtrsim 12.5$ ns yields unproportional signal

Machine Learning: Network Architecture

- Deep Neural Network (DNN)
  - Tool
    - **Keras** with **TensorFlow**
  - Architecture
    - Four hidden layers with 64/64/128/256 nodes using a $\tanh(x) + 1$ or swish activation
    - One linear layer with one node
  - Loss metric
    - Mean Absolute Error (MAE) initially, now using Leaky Gaussian Kernel
    - Optimization algorithm ADAM
  - Hyperparameters (explorations mostly ongoing).
    - 100 epochs for training
    - Learning rates 0.001

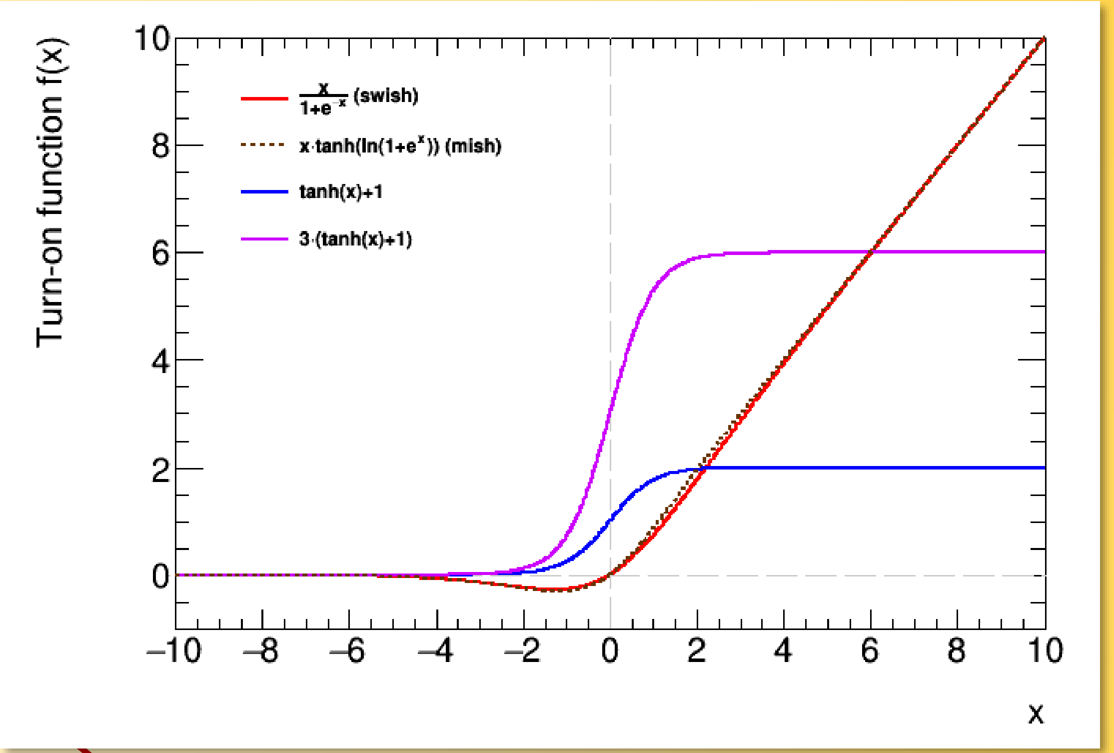

$$-\frac{1}{\sqrt{\alpha\cdot\pi/2}}\exp\left(-\frac{(x-x_{\mathrm{target}})^2}{2\alpha^2}\right)+\beta\cdot|x-x_{\mathrm{target}}|$$